Inter-comparison of dynamic models for radionuclide transfer to marine biota in a Fukushima accident scenario ☆

J. Vives i Batlle [a, *], N.A. Beresford [b], K. Beaugelin-Seiller [c], R. Bezhenar [d], J. Brown [e], J.-J. Cheng [f], M. Ćujić [g], S. Dragović [h], C. Duffa [c], B. Fiévet [c], A. Hosseini [e], K.T. Jung [i], S. Kamboj [f], D.-K. Keum [j], A. Kryshev [k], D. LePoire [f], V. Maderich [d], B.-I. Min [j], R. Periáñez [l], T. Sazykina [k], K.-S. Suh [j], C. Yu [f], C. Wang [f], R. Heling [m, 1]

[a] Belgian Nuclear Research Centre (SCK•CEN), Boeretang 200, 2400 Mol, Belgium
[b] NERC – Centre for Ecology & Hydrology, Library Avenue, Lancaster, LA1 4AP, UK
[c] Institut de Radioprotection et de Sûreté Nucléaire (IRSN), PRP-ENV, France
[d] Institute of Mathematical Machine and System Problems, Glushkov Av., 42, Kiev 03187, Ukraine
[e] Norwegian Radiation Protection Authority, Grini Næringspark 13, P.O. Box 55, NO-1332 Østerås, Norway
[f] Argonne National Laboratory, Environmental Science Division, 9700 South Cass Avenue, EVS/Bldg 240, Argonne, IL 60439, USA
[g] University of Belgrade, Institute for the Application of Nuclear Energy, Banatska 31b, 11080 Belgrade, Serbia
[h] Vinča Institute of Nuclear Sciences, University of Belgrade, P.O. Box 522, Belgrade, Serbia
[i] Korea Institute of Ocean Science and Technology, 787, Haean-ro, Ansan 426-744, Republic of Korea
[j] KAERI – Korea Atomic Energy Research Institute, 150 Deokjindong, Yu Song, P.O. Box 105, 305-353 Daejeon, Republic of Korea
[k] Research and Production Association "Typhoon", 4 Pobedy Str., Obninsk, Kaluga Region 249038, Russia
[l] Departamento de Física Aplicada I, University of Seville, Carretera de Utrera km 1, 41013 Seville, Spain
[m] NRG, Utrechtseweg 310, 6800 ES Arnhem, The Netherlands

A B S T R A C T

We report an inter-comparison of eight models designed to predict the radiological exposure of radio-nuclides in marine biota. The models were required to simulate dynamically the uptake and turnover of radionuclides by marine organisms.

Model predictions of radionuclide uptake and turnover using kinetic calculations based on biological half-life ($T_{B1/2}$) and/or more complex metabolic modelling approaches were used to predict activity concentrations and, consequently, dose rates of ^{90}Sr, ^{131}I and ^{137}Cs to fish, crustaceans, macroalgae and molluscs under circumstances where the water concentrations are changing with time. For comparison, the ERICA Tool, a model commonly used in environmental assessment, and which uses equilibrium concentration ratios, was also used. As input to the models we used hydrodynamic forecasts of water and sediment activity concentrations using a simulated scenario reflecting the Fukushima accident releases.

Although model variability is important, the intercomparison gives logical results, in that the dynamic models predict consistently a pattern of delayed rise of activity concentration in biota and slow decline instead of the instantaneous equilibrium with the activity concentration in seawater predicted by the ERICA Tool. The differences between ERICA and the dynamic models increase the shorter the $T_{B1/2}$ be-comes; however, there is significant variability between models, underpinned by parameter and methodological differences between them.

The need to validate the dynamic models used in this intercomparison has been highlighted, partic-ularly in regards to optimisation of the model biokinetic parameters.

Keywords:
Dynamic model
Dose rate
Fukushima
Marine biota
Radionuclide transfer
MODARIA

1. Introduction

Radiological protection of the environment (i.e. wildlife) is still relatively novel and exposure assessment methodologies for non-human biota are being continually improved. It is generally

☆ This paper is dedicated to the memory of our departed colleague and friend Rudie Heling.

* Corresponding author.
E-mail address: jordi.vives.i.batlle@sckcen.be (J. Vives i Batlle).

[1] Deceased.

accepted that prediction of the uptake of radionuclides from the surrounding environmental media by organisms is a major source of uncertainty (Beresford et al., 2008).

The development of assessment approaches has focused on chronic exposure scenarios and, for aquatic biota, the majority of radiological assessment models assume that the activity concentration in an organism of mass M (i.e. A_O, in Bq kg^{-1} expressed on a fresh mass (f.m.) basis) is proportional to the activity concentration (A_W, in Bq L^{-1}) in an adjacent volume V of water *via* a whole organism concentration ratio, or CR_{wo} (in L kg^{-1} f.m.) (IAEA, 2014). The ERICA Tool (Brown et al., 2008) is an example of a model which represents the uptake of radionuclides from environmental media by these simple CR_{wo}s. These methodologies are unlikely to assess reliably situations outside of equilibrium.

The truth is that, in reality, instantaneous equilibrium between biota and the medium does not exist. This is because biota accumulates radionuclides with a 'time delay' relative to variations of activity concentration in seawater. In its simplest formulation, the dynamics of the process are determined by a balance between the residence time of the radionuclide in the water in the presence of efficient hydraulic dilution, and the biological half-life ($T_{B1/2}$) of an organism. For a single component biological half-life, the activity concentrations in biota (A_O, Bq kg^{-1}) and water (A_W, Bq m^{-3}) can be represented by a simple model with two rate constants; k_W for uptake and k_O for elimination: $\frac{dA_O}{dt} = \mathrm{k}_W A_W \frac{V}{M} - (\mathrm{k}_O + \lambda)A_O$; $\frac{dA_W}{dt} = -(\mathrm{k}_W + \lambda)A_W + \mathrm{k}_O \frac{M}{V} A_O$.

Where $k_O = \frac{\ln 2}{T_{B1/2}}$, $k_W = ((k_O + \lambda)M/V)CR_{wo}$ and λ is the radionuclide decay constant (Vives i Batlle, 2012). This type of model can be simplified by assuming that the water concentration does not depend on the exchange from an aquatic organism (because the amount of radioactivity in the organism is much smaller than in the surrounding volume of water, V) – hence $dA_W/dt \approx 0$, and that the organism uptake rate does not change with time (i.e. ignoring the effect of organism growth).

Other dynamic models exist that are more complex and can, for example, model uptake by higher organisms *via* food (Brown et al., 2004; Keum et al., 2015; Maderich et al., 2014), requiring two additional parameters: assimilation efficiency and ingestion rate. Furthermore, some models consider organism growth processes requiring information on metabolism (Sazykina, 2000) and other models include more complex food web modelling (Heling et al., 2002).

The Fukushima nuclear accident has refocused strongly the vision for marine radioecology and highlighted the limited knowledge that we have in this area (Vives i Batlle, 2011). This disaster has brought some evidence that a dynamic modelling approach is advantageous compared with traditional equilibrium-based transfer approaches (Psaltaki et al., 2013; UNSCEAR, 2014; Vives i Batlle et al., 2014; Vives i Batlle and Vandenhove, 2014), owing to the relatively slow response of many biota to changing concentrations in seawater. Some models such as BURN-POSEIDON (Maderich et al., 2014), D-DAT (Vives i Batlle et al., 2008) and ECOMOD (Sazykina, 2000) have been applied in a 'dynamic assessment' context, including as part of the recent assessments of the impact of the Fukushima nuclear accident on marine biota in the acute phase (Tateda et al., 2013; Vives i Batlle et al., 2014), closely following initial application of equilibrium models to make predictions (Garnier-Laplace et al., 2011).

Notwithstanding the availability of some models for dynamic situations, the availability of parameterisation data is a problem. There are many knowledge gaps, especially concerning elemental biological half-lives, and there are several types of model in use ranging from simple linear first order kinetic approaches to metabolic and foodchain transfer models. To date, there has been no international comparison of dynamic models for estimating biota exposure. For this reason, we decided to perform the first systematic comparison between such models within the International Atomic Energy Agency (IAEA) MODARIA programme (http://www-ns.iaea.org/projects/modaria/default.asp).

The focus of this study was to compare activity concentrations and exposures to biota calculated by dynamic transfer models; the location chosen for this model simulation was close to the point where radionuclides were released from the Fukushima Nuclear Power Plant to the Pacific Ocean during the reactor accident in March/April 2011. We used seven dynamic models: BURN-POSEIDON, the ANL approach, D-DAT, ECOMOD, the IRSN approach, K-BIOTA-DYN-M and the NRPA marine dynamic model; all models are described and referenced in Section 2.1 below. The predictions of these dynamic models were compared with the output from the equilibrium-based ERICA Tool. The input for the intercomparison was a series of hydrodynamic forecasts or monitoring data (activity concentrations in seawater and sediment) for a site close to the Fukushima nuclear complex for the 110 days after the accident, produced by means of marine dispersion models, as referenced below.

The resultant estimates should be considered as illustrative only, and not as a thorough assessment of exposures and effects at this site close to the Fukushima NPP. Such an evaluation using both model prediction and monitoring measurements can be found elsewhere (Vives i Batlle et al., 2014). The present study is based on model comparisons for a single location in close proximity to the release point, and thus the calculated activity concentrations in water and sediments used in the present study represent only a limited area. This area is not representative of the general region inhabited by populations of biota, since the gradients of the activity concentrations for both water and sediments are very pronounced (UNSCEAR, 2014). This is why the discussion of the results is limited to the numerical differences between the models and does not include an evaluation of the levels of exposures and possible effects on biota.

2. Materials and methods

2.1. Input data for the intercomparison

The inputs to the exercise were the modelled activity concentrations of ^{90}Sr, ^{131}I, and ^{137}Cs in near-surface water (top 1 m; Bq m^{-3}) as well as bottom seawater (Bq m^{-3}) and sediment (Bq kg^{-1}, dry mass – d.m.) given at daily intervals. The period of the simulation was fixed between 11 March and the end of June 2011 (^{90}Sr) and July (other two radionuclides), owing to the different setup of the model employed for ^{90}Sr. The radionuclide concentrations were obtained from a suite of marine dispersion models that have been previously validated and compared (Periáñez et al., 2015). Lagrangian models were used for ^{137}Cs and ^{131}I (Kawamura et al., 2011; Min et al., 2013) and an Eulerian model was applied in the case of ^{90}Sr (Periáñez et al., 2013). Essentially, these models utilise current fields pre-computed by operative three-dimensional hydrodynamic models to solve the transport of radionuclides in the sea. This is determined by advection due to currents and turbulent mixing. Interactions of radionuclides with sediments are described in a dynamic way, in terms of kinetic transfer coefficients. Both direct releases into the Pacific Ocean and deposition from the atmosphere were used as modelling source terms for each radionuclide.

For ^{131}I and ^{137}Cs, the model simulations were based on the source term estimated by the Japan Atomic Energy Agency (JAEA) from measurements made by the Tokyo Electric Power Company (TEPCO) at the point of discharge (Periáñez et al., 2015). In the case of ^{90}Sr, an inverse modelling technique was used to estimate the

source from marine surface water measurements, complemented with several vertical profiles in various parts of the ocean (Kawamura et al., 2011; Min et al., 2013; Periáñez et al., 2013). The outputs generated, which have been validated and are supposed to give realistic results, were given at continuous daily intervals for a coastal station situated 30 m north of the Dai-ichi drainage channels: 37° 25′ 51″ N, 141° 2′ 3″ E.

The data used in this exercise are not based on measured activity concentrations (water and sediment), contrary to the recent UNSCEAR assessment (UNSCEAR, 2014). Instead, they are based on the outputs of the hydrodynamic model simulations. This approach was chosen because the continuous nature of the hydrodynamic simulations facilitates application of the biological transfer models: the discrete nature of the actual measurements would have resulted in input data at irregular time intervals, requiring interpolation for some models, thus adding an unnecessary layer of variability to the intercomparison.

2.2. Description of models participating in the benchmark scenario

2.2.1. BURN-POSEIDON approach (NRG/IMMSP/KIOST)[2]

The biota model used in the compartment model POSEIDON-R (Lepicard et al., 2004) is the simplified dynamic food web model BURN (Heling et al., 2002). In the BURN-POSEIDON model, marine organisms are grouped into a limited number of classes based on their trophic level and type of species: phytoplankton, zooplankton, fishes (two types: piscivorous and non-piscivorous), crustaceans (e.g. detritus-feeders), and molluscs (filter-feeders). Given that BURN gives results for two types of fish (piscivorous and non-piscivorous), we averaged these and treated the result as 'pelagic fish' for comparison purposes. There are no benthic fish predictions for this model.

All organisms are considered to take up radionuclides directly from water as well as *via* food. Due to their relatively rapid uptake and short retention time (Vives i Batlle et al., 2008), the concentrations of radionuclides in phytoplankton are calculated using the concentration factor approach. The differential equations for the rest of marine organisms describe intake from food, from water and elimination of radionuclides (Maderich et al., 2014). The basic equation connecting concentration of activity in predator C_{pred} with concentration in food C_f and in water is: C_w is $\frac{dC_{pred}}{dt} = aK_1C_f + bK_WC_W - k_bC_{pred}$, where t is time, K_1 is the food uptake rate, a is the coefficient for radionuclide transfer through food, K_w is the water uptake rate, b is coefficient for radionuclide transfer to tissue from water and k_b is the fish body elimination rate. The parameter b includes implicitly all processes for extraction of radionuclides from water including water passing the gills, water inadvertently passing through the gut and water absorbed from gills, gut and skin.

In fishes, where radioactivity is not homogeneously distributed over all the tissues of the organism, it is assumed that the radionuclide accumulates in a specific tissue (target tissue). This tissue (bone, flesh, stomach, or organs) controls the $T_{B1/2}$ in the organism. The above equation applies to the target tissue. The radioactivity concentration in the fish body is then obtained from the concentration in the target tissue diluted by the remaining body mass of the fish.

The BURN model has recently been extended to include the benthic food web. A preliminary comparison carried out separately from this study does not show large differences between pelagic predator fish and benthic predator fish within 15 km off the Fukushima complex during the first year after Fukushima accident (contrary to demersal fish which feeds on the sediments). Therefore, there is an indication that piscivorous fish can be a reasonable approximation for benthic predatory fishes (V. Maderich, pers. comm.).

2.2.2. ANL approach (ANL)

To model the radionuclide concentration in an aquatic organism with changing adjacent water concentrations, the ANL approach assumes that the radionuclide concentration in the organism is zero before the start of effluent releases and is related to water concentration after the start of the releases by a simple kinetic model that considers uptake and elimination of radionuclides by the organism. The governing equation for the amount of radionuclide in the organism and water, A_o and A_w in this classical kinetic model, $\frac{dA_O}{dt} = k_WA_W - (k_O + \lambda)A_O$, is again that of a single component of uptake and a single component of loss, represented by two rate constants – k_W for uptake and k_O for elimination. This type of model requires knowledge of the $T_{B1/2}$ and the CR_{wo}. The latter is required because, at equilibrium, $dA_O/dt = 0$, whereupon $A_W/A_O = (k_O + \lambda)/k_W$ and A_W/A_O is directly linked to the CR_{wo}.

To solve the model equations, the ANL approach uses numerical discretisation, leading to $A_0(t_{n+1}) = e^{-(k_0+\lambda)t_{n+1}} \int_{t_n}^{t_{n+1}} e^{(k_0+\lambda)\tau}k_wA_w(\tau)d\tau + A_0(t_n)e^{-(k_0+\lambda)(t_{n+1}-t_n)}$, where t_{n+1} is the next discrete time step after t_n and τ is the continuous time variable over which the integration between the discrete time steps is performed. Defining $\Delta t = t_{n+1} - t_n$, $A_0^{n+1} = k_w \cdot \Delta t \cdot A_w^{n+1} + A_0^n e^{-(k_0+\lambda)\Delta t}$, the activity concentration in the organism at the next time step is equal to the amount of activity uptake $k_wA_w\Delta t$ and the amount of activity remaining from the previous time step (i.e., after subtracting what is excreted through biological processes and lost through decay).

2.2.3. D-DAT approach (SCK•CEN)

The D-DAT dynamic model was previously described both in terms of its functionality (Vives Batlle et al., 2008) and its application to the Fukushima releases (Vives i Batlle et al., 2014; Vives i Batlle and Vandenhove, 2014). The associated biokinetic – allometric data for ^{131}I and ^{134,137}Cs were also reported previously (Vives i Batlle et al., 2007b). Essentially, D-DAT uses similar equations to the ANL approach described above, though D-DAT is set-up within the modelling software *ModelMaker* (Citra, 1997; Rigas, 2000) which solves equations numerically using the Gear integration method (Gear, 1971).

For the present study, the model (which in its most general form uses a dual-component $T_{B1/2}$) was used in a single component version, whereupon the governing equations for the activity concentration (per unit mass for biota and volume for water), A_0 and A_w, reduce to a simple two-compartment model with two rate constants; k_w for uptake and k_O for elimination: $\frac{dA_O}{dt} = k_WA_W\frac{V}{M} - (k_O + \lambda)A_O$; $\frac{dA_W}{dt} = -(k_W + \lambda)A_W + k_O\frac{M}{V}A_O$, where $k_O = \frac{\ln 2}{T_{B1/2}}$, $k_W = ((k_O + \lambda)M/V)CR$, λ is the radionuclide decay constant, M is the mass of the organism and V is the volume of water surrounding the organism (Vives i Batlle, 2012). In reality, A_W does not change significantly as a result of the exchange with the biota because V is generally much larger numerically than M.

The model solution for $A_W(t)$ is calculated by "forcing" the supplied hydrodynamic data onto dA_W/dt (the derivative of the seawater concentration, calculated using the central three-point method of numerical differentiation), linearly interpolating in places where input values are not available in consecutive time steps. The model then checks that the numerical integral of the compartment equation up to a given time τ after N discrete steps of length Δt, $\sum_{i=1}^{N}\frac{dA_W(t_i)}{dt}\Delta t$, is sufficiently close to the available activity

[2] Organisations running the models for this exercise are shown in parenthesis.

concentration $A_W(\tau)$. The last step is the calculation of internal and external exposure, using dose conversion coefficients (DCCs), which are the dose rate per unit activity concentrations (in units of μGy h^{-1} per Bq kg^{-1} organism or media, respectively) for marine reference organisms, taken from the ERICA approach (Brown et al., 2008).

2.2.4. ECOMOD approach (Spa Typhoon)

ECOMOD is a dynamic model which utilises stable chemical analogues and ratios of radionuclides to determine the concentrations of radionuclides in aquatic biota (Sazykina, 2003, 2000). It is based on two main principles, namely that: (a) stable and radioactive isotopes with identical or similar chemical properties form a common "pool" of the element; and (b) the elemental chemical composition of biomass for each biological species is unique and constant (Liebig, 1847; Vernadsky, 1929). To produce one unit of new biomass, an organism 'consumes' from the environment specified amounts of particular elements.

The model as described in Sazykina (2000) has equations that describe the transfer of chemical (biogenic) elements from the environment to the food chains of organisms and back to the environment (ecological cycles of elements). From this, these authors derived an equation for the activity concentration $y(t)$ in the biomass: $\frac{dy}{dt} = [G(t) + \varepsilon_A \times B(t)](CR_{wo} \times X - y) - \lambda y$, where $B(t)$ is the biomass loss due to metabolic processes, ε_A indicates the loss of a radionuclide in metabolic processes, $G(t)$ is the biomass production, X is the activity concentration of the radionuclide in the medium and λ is the radioactive decay constant. In the simplest case in which the biomass is constant and the activity concentration in the environment is also constant, $y(0) = 0$ and decay can be ignored ($\lambda \cong 0$), the equations have an analytical solution of the form $y(t) = X \times CR_{wo} \times (1 - e^{-pt})$ where $CR_{wo} = Q^A{}_1/Q^A{}_0$ for the element A and p is defined as $p = G(t) + \varepsilon_A B(t)$. Such an equation is the simplest formula of the dynamics of radionuclide accumulation in the biomass of a population (Polikarpov, 1965; Whicker and Schultz, 1982).

2.2.5. IRSN approach (IRSN)

The IRSN dynamic modelling approach also implements first-order kinetic parameters to calculate transfers on the basis of time-series measurements or hydrodynamic model predictions for the medium. The full transfer model is thoroughly described elsewhere (Fievet and Plet, 2003; Fiévet et al., 2006). Basically, radionuclide transfers between seawater and a biological compartment are classically depicted considering $A_w(t)$ and $A_o(t)$, the radionuclide activity concentrations outside and inside the biological compartment, as a function of time (t), taking into account the rate constants for the radionuclide input and output, respectively noted k_w and k_o. Only two transfer parameters CR_{wo} and $T_{B1/2}$ are required to calculate the changes in the radionuclide concentration in the biological compartment as a response to the changes in seawater, with respect to the transfer kinetics.

The time series concentration in seawater determines the concentration in the biological compartment in very much the same way as described for the ANL and D-DAT models. The sampling period is $T = t(i+1) - t(i)$. The relationship between $A_w(i)$ and $A_o(i)$, is depicted by the equation: $A_o(i) = a \times s(i) - 1) + b \times A_w(i)$, where $A_o(i)$ is the concentration inside the (biological) compartment at step i = time $t(i)$, $A_w(i)$ is the concentration outside (seawater) at step i = time $t(i)$ and where a and b are the parameters depending on CR, $T_{1/2}$ (the decay half-life of the radionuclide) $T_{B1/2}$ (the biological half-life) and T (the time interval between step i and step $i-1$).

The values of CR_{wo} and $T_{B1/2}$ are obtained from the literature or derived directly from field measurement data (Fievet and Plet, 2003). This introduces some element of data selection in the comparison, rather than just comparing model formulation. We discuss explicitly any instances in which this makes a significant a difference in the results.

Activity concentrations in water, sediment and organisms are used to assess internal and external dose rates to biota, using dosimetry factors for marine organisms calculated with the EDEN approach (Beaugelin-Seiller et al., 2006), according to the scenario specifications.

2.2.6. K-BIOTA-DYN-M approach (KAERI)

K-BIOTA-DYN-M is a dynamic compartment model consisting of seven compartments: phytoplankton, zooplankton, prey fish, benthic fish, crustacean, mollusc, and macroalgae. The phytoplankton compartment is assumed to be instantaneously in equilibrium with the seawater, and thus its activity concentration is estimated using the CR_{wo}. The other compartments intake radioactivity from both water and food (except for algae), and lose radioactivity *via* biological elimination and radioactive decay.

The model is described in detail elsewhere (Keum et al., 2015). Essentially, radioactivity intake *via* water (FP_{wj}) is modelled as $FP_{wj} = k_{wj}A_w(t)$ whereas radioactivity intake *via* food j (FP_j) is modelled as $FP_j(t) = f_jA_j(t)\tau I_{food}$ where k_{wj} is the water uptake rate of biota, f_j is the contribution of food j to the total food consumption, A_j is the activity concentration of food j, I_{food} the daily feeding rate and τ the assimilation efficiency of the radionuclide from food. The activity balance equations for biota are as follows:

$$\text{Phytoplankton and zooplankton}: A_o = CR_{phy}A_w;\ \frac{dA_1}{dt} = \phi_{w1} + \phi_0 - (\lambda + k_{b1})A_1$$

$$\text{Prey and predator fish (benthic or pelagic)}: \frac{dA_2}{dt} = \phi_{w2} + \phi_1 - (\lambda + k_{b2})A_2;\ \frac{dA_3}{dt} = \phi_3 + \phi_2 + \phi_8 - (\lambda + k_{b3})A_3$$

$$\text{Crustacean, mollusc and macroalgae}: \frac{dA_4}{dt} = \phi_{w4} + \phi_3 + \phi_5 + \phi_6 + \phi_9 - (\lambda + k_{b4})A_4;\ \frac{dA_5}{dt} = \phi_{w5} + \phi_4 + \phi_7 - (\lambda + k_{b5})A_5;\ \frac{dA_6}{dt} = \phi_{w6} - (\lambda + k_{b6})A_6$$

where CR_{phy} is the CR_{wo} for phytoplankton, $A_w(t)$ is the seawater activity concentration at time t, $A_o(t) - A_6(t)$ are the activity concentrations of biota (sub-indices for phytoplankton, zooplankton, prey fish, predator fish, crustacean, mollusc and macroalgae) at time t, $\phi_{w1}(t) - \phi_{w6}(t)$ and $\phi_0(t) - \phi_9(t)$ the radionuclide intake rate from water and food per unit mass of biota, respectively, with the suffixes suffix 1–6 for water and 1–9 for food, labelling the different flows interconnecting the model compartments; λ is the radionuclide decay rate (d^{-1}) and $k_{b1} - k_{b6}$ are the biological elimination rates.

2.2.7. NRPA marine dynamic model (NRPA)

The NRPA marine dynamic model (Brown et al., 2004), based on previous work (Fisher, 2002; Landrum et al., 1992; Thomann, 1981), considers uptake *via* food and water for aquatic organisms. Elimination rates are assumed to be independent of the uptake route, the assimilation efficiency is assumed to be independent of food type, and predators are assumed not to assimilate the activity in the gut content of their prey. Further assumptions are that the zooplankton

is a homogeneous group, described by generic radioecological parameter values, and that the growth rate for all organisms is zero.

The starting point for the simulation is taken as the entry of radionuclides into the food-chain for assumed fish prey organisms (zooplankton or mollusc). For zooplankton and mollusc, equilibrium with the water concentration is assumed, using the CR_{wo} approach. For fish (uptake *via* water and food), the dynamic equation is $dC_f/dt = AE_f IR_f C_p + k_{uf} C_w - C_f k_{ef}$, where AE_f is the assimilation efficiency (dimensionless) for fish, IR_f is the ingestion rate per unit mass, C_p is the activity concentration in prey, k_{uf} is the uptake rate of radionuclide to fish directly from the water column, C_w is the concentration in water, C_f is the activity concentration in fish and k_{ef} is the depuration rate. CR_{wo} values (arithmetic means) for zooplankton and mollusc have been taken from IAEA TRS 479 (2014), fish depuration rates (based on biological half-lives) from ICRP Publication 114 (2009); all other parameters for ^{137}Cs having being taken from Thomann (1981). Loss rates for ^{90}Sr were based on the allometric relationships given by Whicker and Shultz (1982).

2.2.8. The ERICA Tool (University of Belgrade, NERC-CEH)

For predictions using an equilibrium model the ERICA Tool (version 1.0; November 2012) as described by Brown et al. (2008) was used. The Tool's default dose conversion factors for the appropriate geometries were used. However, where available, CR_{wo}s were sourced from the 2013 version of the 'Wildlife Transfer Database' (WTD) as described by Copplestone et al. (2013) rather than using the Tool's default values. The values used from the WTD were the arithmetic means as subsequently published in IAEA (2014). Note that the CR_{wo} values used in the ERICA Tool (v1.0) or presented in IAEA (2014) were also applied by some models because these were the more comprehensive CR_{wo} datasets available at the time of the work. Any instances in which this made a significant difference in the comparison results are explicitly discussed.

The WTD did not contain CR_{wo} values for iodine transfer to fish or crustaceans in the marine environment. For fish, the I CR_{wo} value was therefore sourced from IAEA Publication 422 (IAEA, 2004), whilst for crustacean the value for Japanese estuaries from the WTD were used (these data were from sites with salinity values similar to marine ecosystems). The CR_{wo} values used are presented in Table 3.

2.3. Intercomparison exercise

The modelled input data were formatted in an Excel spreadsheet which also formed the results template provided to participants. Each model was run singly (along with their own parameters, such as biological half-lives) with the exception of the ERICA Tool, which was run by two collaborating participants (University of Belgrade in collaboration with one of the Tool's developers, NERC-CEH).

Table 1
Definition of reference organisms considered as ellipsoids (these are the default geometries from the ERICA Tool).

Organism	Mass (kg)	Length (cm)	Width (cm)	Height (cm)
Benthic fish	1.31E+00	3.99E+01	2.49E+01	2.51E+00
Pelagic fish	5.65E−01	3.00E+01	6.00E+00	6.00E+00
Crustacean	7.54E−01	2.00E+01	1.20E+01	6.00E+00
Benthic mollusc	1.64E−02	5.00E+00	2.50E+00	2.50E+00
Macroalgae	6.54E−03	5.00E+01	5.00E−01	5.00E−01

Note: The ERICA macroalgae geometry at the time the exercise was initiated had dimensions of 50 × 0.5 × 0.5 cm and mass 6.54 g. This was different from the ICRP brown seaweed which is considered to have dimensions of 50 × 50 × 0.5 cm and mass of 652 g. For this exercise, we adhered to the original ERICA Tool definition (note version 1.2 of the ERICA Tool has the same geometry as specified in ICRP (2008)).

Table 2
Occupancy factors for the reference organisms (defaults from the ERICA Tool).

Habitat	Benth. fish	Pel. fish	Crustacean	Mollusc	Macroalgae
Water-surface	0	0	0	0	0
Water bottom	0	1	0	0	0
Sediment-surface	1	0	1	1	1
Sediment	0	0	0	0	0

By applying the modelled activity concentrations in seawater and sediment, the dynamic models were able to predict activity concentrations in the following organisms: pelagic fish, benthic fish, crustaceans, molluscs and macroalgae. The organisms were specified to have the same dimensions and occupancy factors as for those defined for the appropriate reference organisms in the ERICA Tool (v1.0) (see Tables 1 and 2). Apart from this, each participant was given the freedom to decide on the biological half-lives, assimilation efficiencies and ingestion rates, CR_{wo}s and dose conversion coefficients to use in the intercomparison. The biokinetic and dosimetry parameters used by each model are detailed in Table 3.

Participants were also offered choice on whether to use surface and/or bottom water data depending on the organism considered (pelagic versus benthic). Most models used the bottom water concentration for benthic fish, molluscs, crustaceans and macroalgae and the surface water concentration for pelagic fish. Following this, participants calculated the whole-organism activity concentrations and associated unweighted internal and external dose rates to the biota in units of μGy h^{-1}, as well as the total dose rate as a function of time (sum of internal and external) and its time integration for 60 days (in μGy^{-1}) following 11 March 2011 to give a cumulative dose estimate for each organism. For models which did not have a dosimetric component, it was suggested that they use the DCC_s from the ERICA Tool (v1.0) to remove additional sources of variability, which were not the focus of the exercise.

2.4. Results interpretation

The interpretation of results focused on identifying differences and similarities in predicted activity concentrations and internal dose rates in biota. This includes an assessment of the time at which the different models predict the maximum activity concentration/dose rate to occur and how quickly these subsequently diminish. Additionally, we focused on analysing differences and similarities between models in respect of integrated doses, attributable to differences in both transfer processes and dosimetry.

In this study, the output of the models *per se* matters less than the differences between the models. No value judgement is passed on whether model predictions lying outside the predictions of the majority of models represent erroneous predictions (or the contrary), as we have no actual data with which to compare these predictions. This study is simply a method of comparing model outputs.

3. Results

Activity concentration, internal and external dose rates for ^{90}Sr, ^{131}I and ^{137}Cs in benthic fish, pelagic fish, crustacean, macroalgae and mollusc are given in Fig. 2 – 6, respectively. Tables 4–8, respectively, relate to the same types of organisms and give the activity concentrations, internal and external dose rates; time of maximum and maximum value of the activity and dose rate; half-time of the slope of the profile in the post-acute period 80–110 days after the accident; and the ratio of the time-integrated dose

Table 3
Biokinetic and dosimetry parameters used by the different applied models.

Param.	Model	^{90}Sr					^{131}I					^{137}Cs				
		Bent. fish	Pel. fish	Crust.	Algae	Mollusc	Bent. fish	Pel. fish	Crust.	Algae	Mollusc	Bent. fish	Pel. fish	Crust.	Algae	Mollusc
$T_{B1/2}$ (days)	BURN-P	N/A	7.5E+02	1.0E+02	N/A	5.0E+01	N/A	8.7E−02	8.7E−02	N/A	8.7E−02	N/A	1.4E+02	1.0E+02	N/A	5.0E+01
	NRPA	6.9E+02	5.6E+02	N/A	N/A	N/A	1.9E+01	1.9E+01	N/A	N/A	N/A	6.5E+01	6.5E+01	N/A	N/A	N/A
	IRSN	1.4E+02	1.4E+02	3.2E+01	1.3E+01	3.2E+01	1.0E+03	1.0E+03	1.0E+03	1.0E+03	1.0E+03	5.0E+01	5.0E+01	1.0E+02	4.0E+01	1.0E+02
	K-BIOTA	1.3E+01	1.3E+01	4.6E+01	4.0E+01	2.3E+01	2.5E−01	2.5E−01	2.9E−01	2.9E−01	1.4E−01	1.3E+01	1.3E+01	4.6E+01	4.0E+01	2.3E+01
	D-DAT	1.4E+02	1.4E+02	2.0E+00	1.3E+01	3.2E+01	3.1E+01	3.1E+01	1.6E+00	5.0E+00	5.6E+01	6.5E+01	6.5E+01	5.8E+01	5.4E+01	1.8E+01
	ANL	4.5E+01	4.5E+01	5.2E+01	3.7E+01	1.2E+01	3.1E+01	3.1E+01	3.0E+01	5.0E+00	4.3E+01	6.5E+01	6.5E+01	7.5E+01	5.4E+01	1.8E+01
CR (L kg^{-1})	BURN-P	N/A	N/A	N/A	1.0E+01	N/A	N/A	N/A	N/A	1.0E+04	N/A	N/A	N/A	N/A	5.0E+01	N/A
	ECOMOD	5.0E+00	5.0E+00	5.0E+01	2.5E+02	1.2E+01	9.0E+00	9.0E+00	1.0E+01	1.0E+03	1.0E+01	4.0E+01	4.0E+01	5.0E+01	5.0E+01	6.0E+01
	NRPA	N/A	N/A	N/A	N/A	8.8E+01	N/A	N/A	N/A	N/A	1.9E+03	N/A	N/A	N/A	N/A	6.3E+01
	IRSN	3.0E+00	3.0E+00	5.0E+00	1.0E+01	1.0E+01	9.0E+00	9.0E+00	3.0E+00	1.0E+04	1.0E+01	1.0E+02	1.0E+02	5.0E+01	5.0E+01	6.0E+01
	D-DAT	2.3E+01	2.3E+01	1.3E+01	4.2E+01	1.2E+02	3.6E+00	3.6E+00	3.6E+00	4.1E+03	1.4E+01	8.6E+01	8.6E+01	4.1E+01	1.2E+02	6.6E+01
	ANL	3.0E+00	3.0E+00	5.0E+00	1.0E+01	1.0E+01	9.0E+00	9.0E+00	3.0E+00	1.0E+04	1.0E+01	1.0E+02	1.0E+02	5.0E+01	5.0E+01	6.0E+01
	ERICA	2.5E+01	2.5E+01	4.9E+01	2.9E+01	1.5E+02	9.0E+00	9.0E+00	3.9E+01	4.2E+03	8.8E+03	8.4E+01	8.4E+01	5.3E+00	9.6E+01	5.0E+01
Assimil. efficiency	BURN-P	N/A	6.0E−01	5.0E−01	N/A	5.0E−01	N/A	6.0E−01	5.0E−01	N/A	5.0E−01	N/A	6.0E−01	5.0E−01	N/A	5.0E−01
	NRPA	3.0E−01	3.0E−01	N/A	N/A	N/A	1.0E+00	1.0E+00	N/A	N/A	N/A	5.0E−01	5.0E−01	N/A	N/A	N/A
	K-BIOTA	6.4E−01	6.4E−01	3.3E−01	N/A	2.8E−01	6.4E−01	6.4E−01	3.3E−01	0.0E+00	2.8E−01	6.4E−01	6.4E−01	3.3E−01	0.0E+00	2.8E−01
Ing. rate (kg d^{-1}/kg)	BURN-P	N/A	1.8E−02	1.5E−03	N/A	6.0E−02	N/A	1.8E−02	1.5e-03	N/A	6.0E−02	N/A	1.8E−02	1.5e-03	N/A	6.0E−02
	NRPA	9.0E−03	9.0E−03	N/A	N/A	N/A	9.0E−03	9.0E−03	N/A	N/A	N/A	9.0E−03	9.0E−03	N/A	N/A	N/A
	K-BIOTA	3.0E−02	3.0E−02	2.7E−02	N/A	6.4E−02	3.0E−02	3.0E−02	2.7E−02	0.0E+00	6.4E−02	3.0E−02	3.0E−02	2.7E−02	0.0E+00	6.4E−02
$DCC_{ext,\ sed}$ (μGy h^{-1} per Bq kg^{-1})	ECOMOD	2.7E−05	N/A	2.3E−05	2.0E−04	7.7E−05	2.0E−04	N/A	1.9E−04	2.3E−04	2.1E−04	2.9E−04	N/A	2.9E−04	3.4E−04	3.2E−04
	NRPA	5.0E−05	N/A	N/A	N/A	N/A	2.0E−04	N/A	N/A	N/A	N/A	3.0E−04	N/A	N/A	N/A	N/A
	IRSN	9.6E−07	N/A	1.9E−07	1.8E−05	9.6E−07	4.0E−05	N/A	2.6E−05	3.8E−05	3.6E−05	6.3E−05	N/A	4.6E−05	5.3E−05	5.0E−05
	K-BIOTA	5.0E−05	N/A	2.8E−05	3.0E−04	8.8E−05	1.3E−04	N/A	1.3E−04	1.0E−04	1.1E−04	3.2E−04	N/A	3.1E−04	3.6E−04	3.4E−04
	D-DAT	5.0E−05	N/A	2.3E−05	2.0E−04	7.7E−05	1.0E−04	N/A	9.5E−05	1.2E−04	1.1E−04	1.5E−04	N/A	1.5E−04	1.7E−04	1.6E−04
	ANL	2.2E−05	N/A	2.2E−05	1.7E−04	6.8E−05	2.0E−04	N/A	2.0E−04	2.2E−04	2.1E−04	2.9E−04	N/A	2.9E−04	3.3E−04	3.2E−04
$DCC_{ext,\ water}$ (μGy h^{-1} per Bq kg^{-1})	BURN-P	2.7E−05	2.7E−05	2.3E−05	1.9E−04	7.7E−05	2.0E−04	2.0E−04	1.9E−04	2.2E−04	2.1E−04	2.9E−04	2.9E−04	2.9E−04	3.3E−04	3.2E−04
	ECOMOD	2.7E−05	2.7E−05	2.3E−05	2.0E−04	7.7E−05	2.0E−04	2.0E−04	1.9E−04	2.3E−04	2.1E−04	2.9E−04	2.9E−04	2.9E−04	3.4E−04	3.2E−04
	NRPA	5.0E−05	2.7E−05	N/A	N/A	N/A	2.0E−04	2.0E−04	N/A	N/A	N/A	3.0E−04	2.9E−04	N/A	N/A	N/A
	IRSN	2.9E−05	2.1E−05	1.6E−05	1.7E−04	4.9E−05	6.9E−05	1.7E−04	8.0E−05	9.0E−05	8.6E−05	1.1E−04	2.5E−04	1.4E−04	1.5E−04	1.2E−04
	K-BIOTA	5.0E−05	5.0E−05	2.8E−05	3.0E−04	8.8E−05	2.0E−04	2.0E−04	1.9E−04	2.3E−04	2.1E−04	3.2E−04	3.2E−04	3.1E−04	3.6E−04	3.4E−04
	D-DAT	5.0E−05	5.0E−05	2.3E−05	2.0E−04	7.7E−05	1.0E−04	1.0E−04	9.5E−05	1.2E−04	1.1E−04	1.5E−04	1.5E−04	1.5E−04	1.7E−04	1.6E−04
	ANL	2.2E−05	2.2E−05	2.2E−05	1.7E−04	6.8E−05	2.0E−04	2.0E−04	2.0E−04	2.2E−04	2.1E−04	2.9E−04	2.9E−04	2.9E−04	3.3E−04	3.2E−04
	ERICA	5.0E−05	2.7E−05	2.3E−05	2.0E−04	2.7E−05	2.0E−04	2.0E−04	1.9E−04	2.3E−04	2.1E−04	3.0E−04	2.9E−04	2.9E−04	3.4E−04	3.2E−04
$DCC_{internal}$ (μGy h^{-1} per Bq kg^{-1})	BURN-P	6.2E−04	6.2E−04	6.3E−04	4.7E−04	5.8E−04	1.3E−04	1.3E−04	1.4E−04	1.1E−04	1.2E−04	1.8E−04	1.8E−04	1.8E−04	1.4E−04	1.5E−04
	ECOMOD	6.2E−04	6.2E−04	6.3E−04	4.5E−04	5.8E−04	1.3E−04	1.3E−04	1.4E−04	1.0E−04	1.2E−04	1.8E−04	1.8E−04	1.8E−04	1.3E−04	1.5E−04
	NRPA	6.0E−04	6.2E−04	N/A	N/A	N/A	1.3E−04	1.3E−04	N/A	N/A	N/A	1.7E−04	1.8E−04	N/A	N/A	N/A
	IRSN	3.6E−04	3.7E−04	3.7E−04	3.1E−04	3.5E−04	8.5E−05	8.7E−05	9.2E−05	7.9E−05	7.3E−05	1.2E−04	1.2E−04	1.3E−04	1.0E−04	9.8E−05
	K-BIOTA	6.0E−04	6.0E−04	6.2E−04	3.5E−04	5.6E−04	1.3E−04	1.3E−04	1.3E−04	1.0E−04	1.1E−04	1.7E−04	1.7E−04	1.8E−04	1.3E−04	1.5E−04
	D-DAT	6.0E−04	6.0E−04	6.3E−04	4.5E−04	5.8E−04	1.3E−04	1.3E−04	1.4E−04	1.0E−04	1.2E−04	1.7E−04	1.7E−04	1.8E−04	1.3E−04	1.5E−04
	ANL	6.3E−04	6.3E−04	6.3E−04	4.8E−04	5.8E−04	1.3E−04	1.3E−04	1.3E−04	1.1E−04	1.2E−04	1.7E−04	1.7E−04	1.7E−04	1.3E−04	1.5E−04
	ERICA	6.0E−04	6.2E−04	6.3E−04	4.5E−04	5.8E−04	1.3E−04	1.3E−04	1.4E−04	1.0E−04	1.2E−04	1.7E−04	1.8E−04	1.8E−04	1.3E−04	1.5E−04

Note: Omits values not used: $T_{B1/2}$ (ECOMOD, ERICA); CR_{wo} (K-BIOTA); $DCC_{ext,\ sediment}$ (BURN, ERICA); assimilation efficiency & ingestion rate (all except BURN, NRPA and K-BIOTA). For BURN, absorption efficiency and ingestion rate are presented as an average for piscivorous and non-piscivorous fish (Maderich et al., 2014).

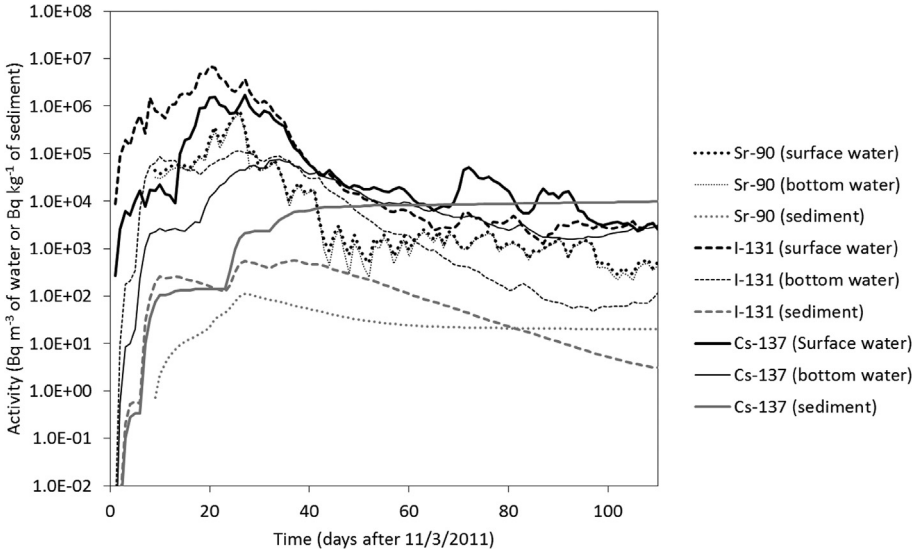

Fig. 1. Modelled seawater and sediment activity concentrations used in this intercomparison.

rate to that derived from the ERICA Tool. The half-time is calculated arbitrarily over a time period of 80–110 days, with the purpose of deriving more accurately an exponential fit for the data well after the discharges had passed their peak. The time-integrated dose is

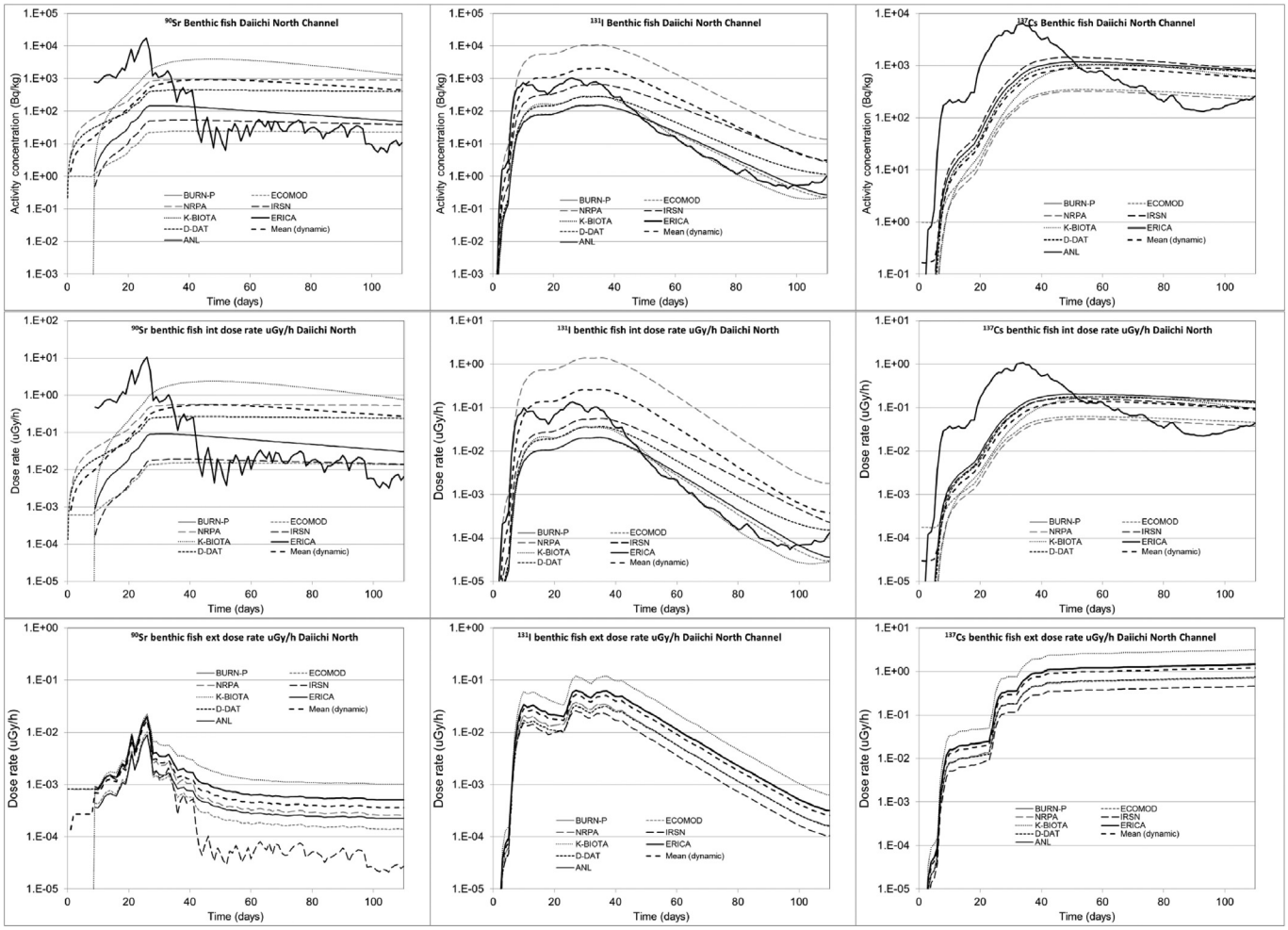

Fig. 2. Activity concentration (top), internal (middle) and external (bottom) dose rate for ^{90}Sr, ^{131}I and ^{137}Cs in benthic fish after 11/3/2011 predicted by the different applied models (there are no predictions for the BURN-P model for benthic fish).

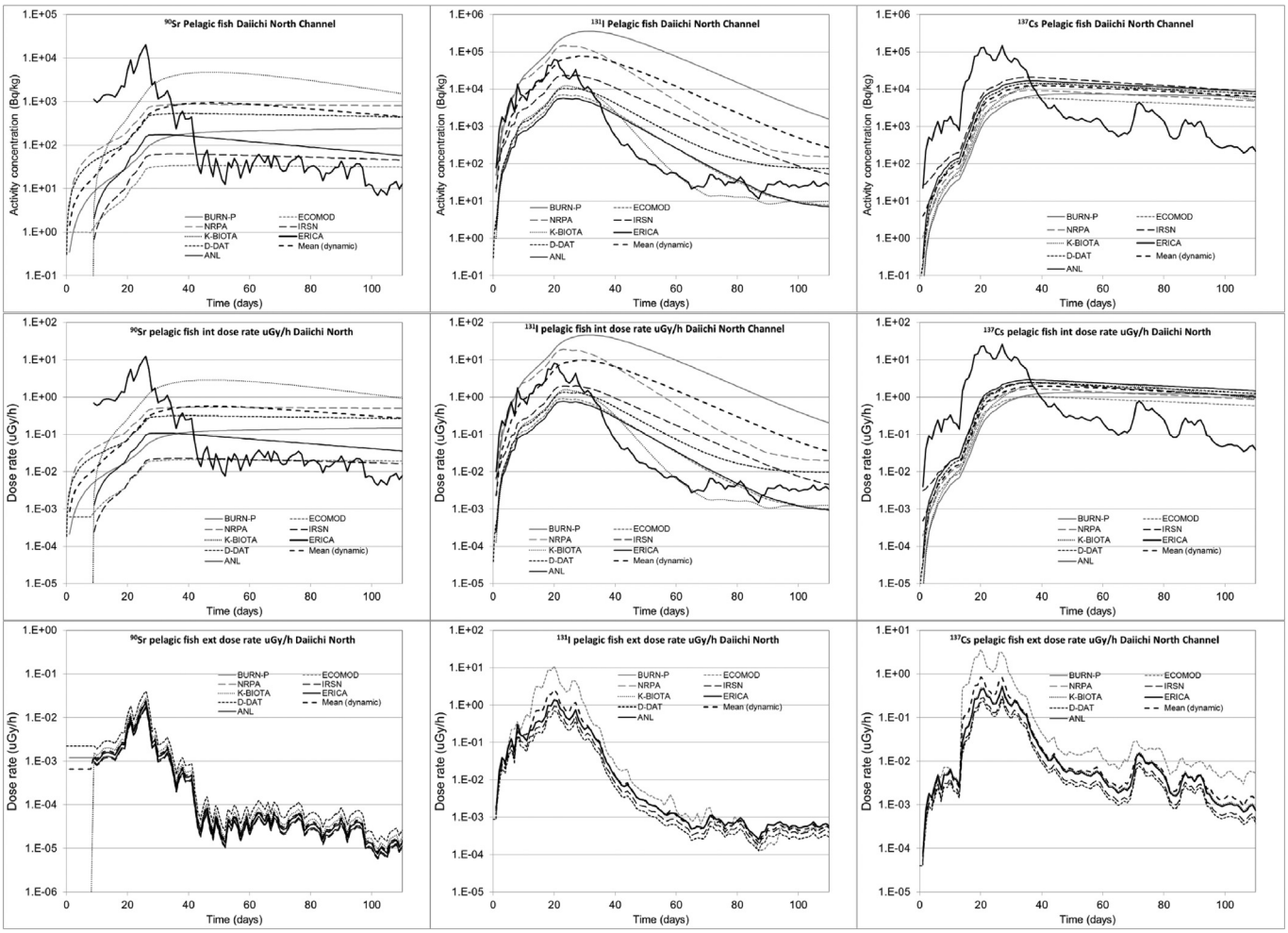

Fig. 3. Activity concentration (top), internal (middle) and external (bottom) dose rate for ^{90}Sr, ^{131}I and ^{137}Cs in pelagic fish after 11/3/2011 predicted by the different applied models.

expressed as a ratio to ERICA in order to focus on how the integration varies relatively, leaving aside concentration ratio effects.

3.1. *Benthic fish*

For ^{90}Sr and ^{131}I, we observe a ~ two-order of magnitude spread in the dynamic model-predicted internal dose rates (reflecting similar variations in activity concentration), whereas for ^{137}Cs the spread is lower (within 1 order of magnitude). For the models that use a CR_{wo} approach, these differences can be attributed to a 1-order of magnitude spread in the CR_{wo}, which determines the maximum concentration that the organism can attain (see Table 3). For models which do not use the CR_{wo} directly (e.g. the NRPA model), the particular values of the alternative approach used, which involves additional parameters such as the ingestion rate and the absorption efficiency, contribute to them giving a different output than the rest.

In the case of ^{90}Sr the highest predicting model is K-BIOTA and the lowest ECOMOD. For ^{131}I the highest is the NRPA model and the lowest is K-BIOTA, the latter decreasing more rapidly than the others because it has the shortest $T_{B1/2}$ of the whole group. For ^{137}Cs, the upper and lower predictions are those for the IRSN and NRPA models, respectively. A number of the models take their iodine CR_{wo} for fish from IAEA (2004); this appears to be for edible tissues entering the human food chain and therefore these models may underestimate whole-body activity concentrations and consequently dose rates.

Model predictions generally decrease exponentially after 30 d for ^{90}Sr and ^{131}I, and 60 d for ^{137}Cs (except for K-BIOTA). This generally reflects the decrease in predicted seawater concentrations past the peak of the accident. However, on close inspection, there is a slight increase of the ^{131}I prediction at the end of the modelling period (e.g. K-BIOTA). This is due to a rise in concentration in the bottom water input data, reflecting the predicted migration of ^{131}I from surface water, which has higher concentrations, to the bottom of the water column where the benthic biota are situated, meaning that the concentration of ^{131}I in the bottom compartment is predicted to be to some extent replenished, due to the high mobility of this radionuclide *via* vertical diffusion (although concentrations at this time are comparatively low).

The variable exponential rate of loss experienced by the models past the discharge peak reflects the rate of decline in seawater concentrations. For the short-lived ^{131}I, the exponential rate of loss has a half-time about 8 d reflecting the radionuclide decay half-life of 8 days. At the opposite end of the range, the mean loss half-time for ^{137}Cs is about 125 d.

The predicted internal dose rates basically mirror the activity concentrations as internal dose is proportional to them. However, there is a slight difference in that, for ^{90}Sr internal dose, the IRSN prediction appears somewhat different to that of the other models with the exception of the ECOMOD model which behaves similarly (see Fig. 2). For the IRSN model, this is likely due to a factor of 2-

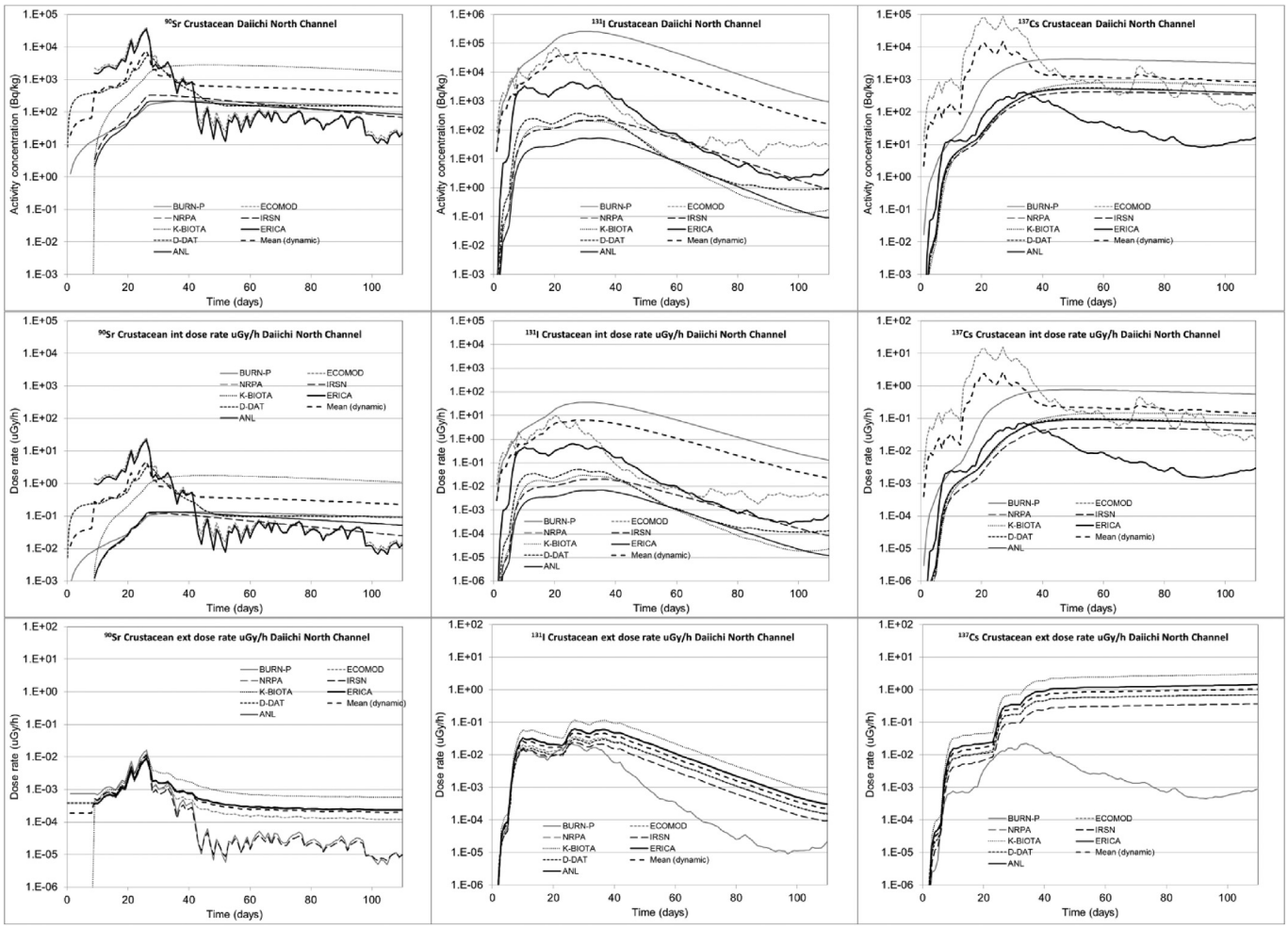

Fig. 4. Activity concentration (top), internal (middle) and external (bottom) dose rate for ^{90}Sr, ^{131}I and ^{137}Cs in crustacean after 11/3/2011 predicted by the different applied models (there are no predictions for the NRPA model for crustacean).

difference between the lower internal exposure DCC's used by IRSN compared with the other models (Table 3). In the case of ECOMOD, no explanation is readily available.

The fact that, for ^{131}I, the NRPA model gives significantly higher dose predictions compared with the other models and the mean dynamic model prediction, requires further explanation. The NRPA approach is one of those models (together with BURN and K-BIOTA) that not only uses a combination of CR_{wo} and $T_{B1/2}$ to determine the kinetic parameters of exchange between water and biota, but also includes food consumption, using the assimilation efficiency and the ingestion rate as well as an uptake rate from the water. For uptake from food, the NRPA model equations include the term $AE_f \times IR_f \times C_p + k_{uf} \times C_w$, where $C_p = CR_p \times C_w$ and the use of a relatively high absorption efficiency for ^{131}I, allied with a relatively high CR_{wo} for the concentration in prey (1.85×10^3 and 0.65×10^3 L kg^{-1} for mollusc and zooplankton, respectively), conspire to give an effectively higher uptake for ^{131}I in benthic fish.

K-BIOTA uses a similar approach as the NRPA model, but has a lower assimilation efficiency and only uses the CR_{wo} approach for phytoplankton, which is perhaps a factor influencing why K-BIOTA predictions are low relative to the NRPA model.

In general, the approaches considering ingestion directly tend to give somewhat higher results than models which do not (e.g. D-DAT, ANL), despite the fact that the CR_{wo} is a compound parameter, implicitly considering the ingestion of food as well as water uptake (ultimately relating both to a 'reference' activity concentration in the medium) in the non-foodchain models. It is rather the combination of high ingestion rate and assimilation efficiency with a conservative assumption that prey at low trophic levels are at equilibrium with the water (a non-dynamic process element) that lies at the root of such differences. The rest of the models (IRSN, ANL and D-DAT) tend to form a 'group'. When this group is considered alone, the variability within models is less than one order of magnitude.

Turning to external dose rates, there is some difference in the temporal pattern of the IRSN model for ^{90}Sr after ~ 40 days, where a profile with sharper variations more akin to the variations in seawater concentrations exists, while the remaining models show a smoother profile. In the region 80–110 days, the profile is very irregular. This generates the low attenuation half-time of 26 days compared with the other models, which are in the order of 150–210 days for that time period (Table 4). One possible factor here is that this model is one of those that consider both water and sediment exposure, but in benthic organisms the external dose rate from sediment exposure begins to dominate over water exposure as water activity concentrations disperse but sediment concentrations are maintained, some 40 days after the accident. Since the IRSN DCC for external exposure from ^{90}Sr in sediment (9.6×10^{-7} μGy h^{-1}) is 50 times below the values for the other models, it is not unexpected that such a difference is observed for

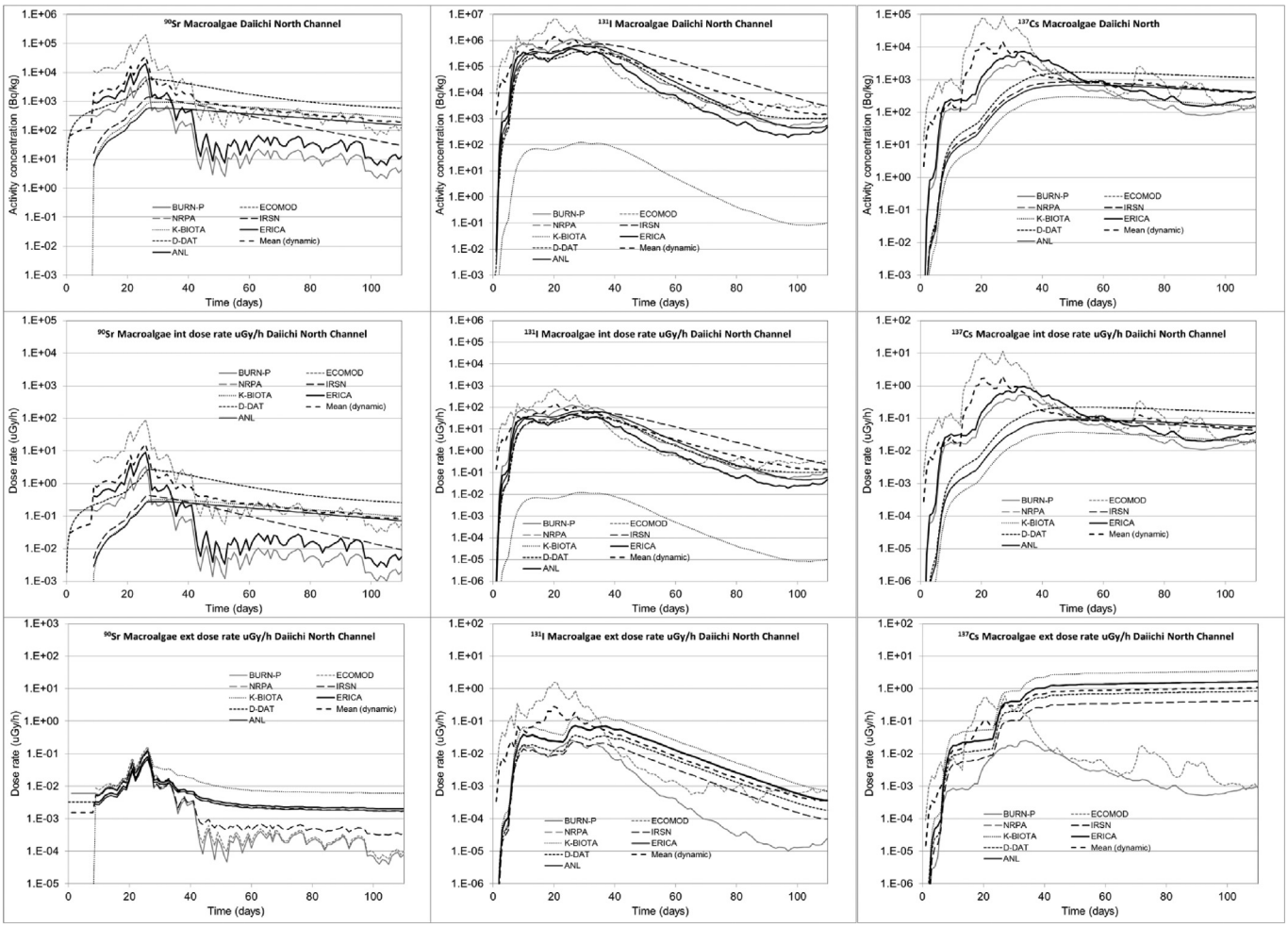

Fig. 5. Activity concentration (top), internal (middle) and external (bottom) dose rate for ^{90}Sr, ^{131}I and ^{137}Cs in macroalgae after 11/3/2011 predicted by the different applied models (there are no predictions for the NRPA model for macroalgae).

that model.

A similar observation can be made for other radionuclides, for the reason that IRSN generally uses lower DCC values for external exposure from sediment than the other models which use external DCCs from ERICA (Table 3). One reason for this difference is that external DCCs from ERICA are the same for both water and sediment. Moreover, organisms are considered as immersed in an infinite medium. The IRSN approach calculates DCCs with regard to sediment and water, taking into account their respective properties in terms of geometry, composition and density. In the present case, organisms are located on a sediment layer of 1 m with a density and composition that differ from those of water. The differential effect would be most noticeable for β-emitters such as ^{90}Sr, explaining the lower values for the IRSN sediment DCC. In addition, the water layer is considered to be 1-m thick rather than infinitely deep. That would result in somewhat lower DCCs for water, which is again as observed in Table 3.

There are additional methodological differences combining to generate variability in external dose rates, with a dispersion of about one order of magnitude in the predicted ^{90}Sr, ^{131}I and ^{137}Cs external dose rates, consistent with the earlier findings reported by Vives i Batlle et al. (2007a; 2011).

For all radionuclides, the dynamic models' external dose calculations generally follow the activity in the water (in the short term) and sediment (increasingly as time progresses and sediment begins to equilibrate with the water). This directly reflects the situation in Fig. 1, where activity concentrations in seawater and sediment "cross" over each other in opposite directions after around 50 days. The predicted external dose rate profile for ^{137}Cs stands out from the rest in that it registers a monotonic increase with time (i.e. the profile does not have a maximum) whereas water concentrations decrease, and thus there is no maximum value (Table 4 reports 110 days as the time of maximum value for the period 80–110 d, and consequently the half-time as negative). This is because, for this radionuclide, the external dose rate is dominated by sediment, and the predicted ^{137}Cs activity concentrations in sediments increased throughout the evaluation period.

3.2. *Pelagic fish*

The results for pelagic fish follow closely those for benthic fish except that the external doses received by these organisms arise from exposure to seawater only (not sediment); the difference is greatest for ^{137}Cs, the radionuclide having the highest sediment-water distribution coefficient (K_d). Activity concentrations of Sr in both surface and bottom water are similar and hence the activity (and internal dose) model predictions for Sr in pelagic fish are very similar to those for benthic fish. For ^{131}I, predictions are one order of magnitude higher than for benthic fish due to higher water concentrations in surface than bottom water.

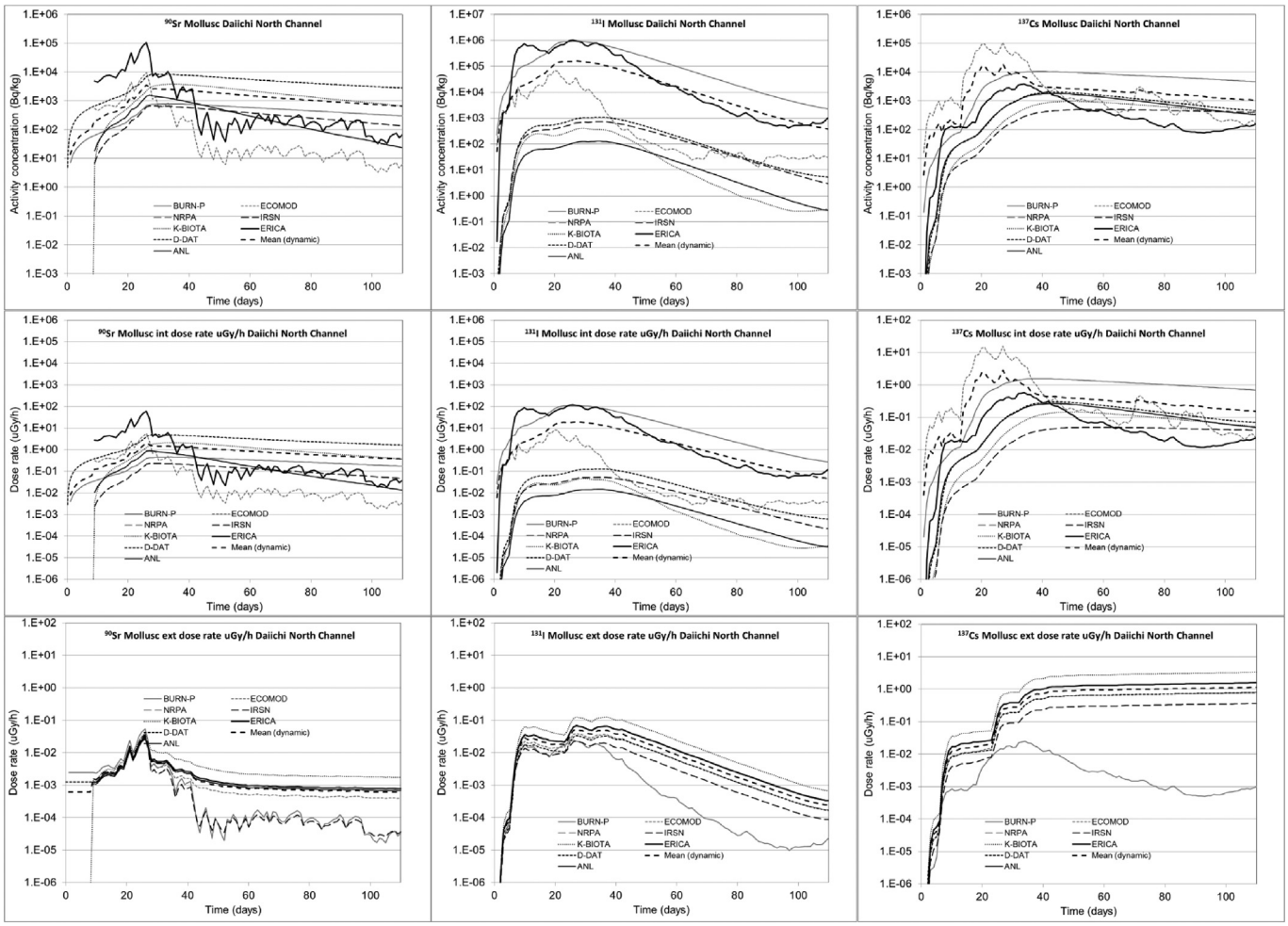

Fig. 6. Activity concentration (top), internal (middle) and external (bottom) dose rate for ^{90}Sr, ^{131}I and ^{137}Cs in mollusc after 11/3/2011 predicted by the different applied models (there are no predictions for the NRPA model for mollusc).

Again, the predicted internal dose rates basically mirror the activity concentrations except for small differences in the IRSN model induced by the fact that the internal DCC for ^{90}Sr and ^{131}I in that approach have factor of two-difference compared with the other models, which use virtually the same DCC as ERICA (Table 3). Although not mentioned further, these observations also apply to the remaining organisms discussed below.

Not unexpectedly, there are some models that give consistently higher activity and internal dose predictions than the dynamic model average, namely, K-BIOTA for ^{90}Sr and BURN/NRPA for ^{131}I. This, again, relates to differences in how the uptake is modelled. Moreover, BURN and NRPA have the highest $T_{B1/2}$ for ^{90}Sr and for this reason the activity concentration does not decrease with time as fast as for the other models. In the case of ^{131}I, differences in $T_{B1/2}$ do not have such a significant effect on the pattern of the results because radioactive decay is the dominant removal process for the radionuclide (in fact, the IRSN model gives the $T_{B1/2}$ an 'artificially high' value of 10^3 days to ignore biological depuration with respect to physical decay). There is, however, still a significant dispersion in the results for ^{131}I activity concentration (and internal dose). The explanation is again that the differences between the highest prediction from BURN and NRPA and the lowest prediction from K-BIOTA are caused by the way they model uptake *via* food directly compared to the application of a CR_{wo} in the other models, whose predictions are more closely clustered. For ^{137}Cs there is high concordance between all the models, with all predictions grouped less than one order of magnitude apart.

The patterns from Table 5 resemble those of Table 4 as already discussed for benthic fish: negative (indicating increase with time in predictions rather than decreases) or long half-time of attenuation for ^{90}Sr and ^{137}Cs in BURN, ECOMOD and NRPA, which form a sub-group, again due to a combination of two factors; relatively high $T_{B1/2}$s and methodological differences in the way ECOMOD calculates transfer. The half-time of attenuation for ^{131}I is unsurprisingly uniform and close to the decay half-life of ^{131}I ($T_{1/2} = 8$ days), again due to the dominance of physical decay over biological elimination.

For external dose, the situation is different from benthic fish due to lack of exposure to sediment, and the models follow the activity in the seawater. For ^{90}Sr and ^{131}I, there is generally tight data grouping and one would only remark that NRPA, K-BIOTA and D-DAT DCC_{ext}s for ^{90}Sr for water exposure are a factor of 2 higher than the rest (consistent with the ERICA Tool) and this is reflected in the dose calculation. Similar differences in DCC_{ext} explain the lower external dose prediction of D-DAT for ^{131}I and ^{137}Cs. Of more significance is that ECOMOD gives higher external dose rate predictions (factor of ~ 4 higher than the average for the dynamic models) for ^{131}I and ^{137}Cs, an intrinsic feature of this model which is difficult to explain as it cannot be correlated to differences in the value of DCC_{ext} or occupancy factors.

Table 4
[a]Activity concentration, internal and external dose rate for ^{90}Sr, ^{131}I and ^{137}Cs in benthic fish: summary of indicator parameters.

Nuclide	Category	Parameter	BURN-P	ECOMOD	NRPA	IRSN	K-BIOTA	D-DAT	ANL	ERICA
^{90}Sr	Activity	T(maximum) (d)	N/A	40	42	35	46	42	33	26
		Maximum (Bq kg^{-1})	N/A	2.5E+01	9.4E+02	5.4E+01	4.0E+03	4.5E+02	1.5E+02	1.8E+04
		Half-time 80–110 d (d)	N/A	500	815	145	30	390	47	14
	Int. dose	T(maximum) (d)	N/A	39	42	35	46	42	33	26
		Maximum (μGy h^{-1})	N/A	1.5E−02	5.7E−01	1.9E−02	2.4E+00	2.7E−01	9.2E−02	1.1E+01
		Half-time 80–110 d (d)	N/A	514	815	145	30	391	47	14
		Integral rel. to ERICA	N/A	2.2E−02	8.4E−01	2.6E−02	2.5E+00	3.9E−01	9.2E−02	1.0E+00
	Ext. dose	T(maximum) (d)	N/A	26	26	26	26	26	26	26
		Maximum (μGy h^{-1})	N/A	1.0E−02	1.9E−02	2.0E−02	2.3E−02	2.0E−02	8.9E−03	2.0E−02
		Half-time 80–110 d (d)	N/A	148	149	26	258	206	210	209
		Integral rel. to ERICA	N/A	4.2E−01	8.0E−01	6.3E−01	1.5E+00	1.0E+00	4.4E−01	1.0E+00
^{131}I	Activity	T(maximum) (d)	N/A	34	35	35	30	35	34	26
		Maximum (Bq kg^{-1})	N/A	1.6E+02	1.1E+04	6.6E+02	2.9E+02	2.8E+02	1.5E+02	1.0E+03
		Half-time 80–110 d (d)	N/A	8	8	9	12	11	8	30
	Int. dose	T(maximum) (d)	N/A	34	35	35	30	35	34	26
		Maximum (μGy h^{-1})	N/A	2.0E−02	1.4E+00	5.6E−02	3.6E−02	3.7E−02	2.1E−02	1.4E−01
		Half-time 80–110 d (d)	N/A	8	8	9	12	11	8	30
		Integral rel. to ERICA	N/A	2.2E−01	1.5E+01	6.5E−01	3.5E−01	4.0E−01	2.3E−01	1.0E+00
	Ext. dose	T(maximum) (d)	N/A	27	27	27	27	27	27	27
		Maximum (μGy h^{-1})	N/A	3.8E−02	3.8E−02	2.6E−02	1.2E−01	3.2E−02	6.3E−02	6.5E−02
		Half-time 80–110 d (d)	N/A	10	10	10	10	10	10	10
		Integral rel. to ERICA	N/A	5.6E−01	5.6E−01	3.8E−01	1.9E+00	5.0E−01	9.8E−01	1.0E+00
^{137}Cs	Activity	T(maximum) (d)	N/A	51	52	50	59	53	51	34
		Maximum (Bq kg^{-1})	N/A	3.5E+02	3.2E+02	1.5E+03	1.1E+03	1.0E+03	1.2E+03	6.5E+03
		Half-time 80–110 d (d)	N/A	99	84	62	40	99	83	−171
	Int. dose	T(maximum) (d)	N/A	51	52	50	61	53	51	34
		Maximum (μGy h^{-1})	N/A	6.3E−02	5.5E−02	1.7E−01	1.8E−01	1.8E−01	2.1E−01	1.1E+00
		Half-time 80–110 d (d)	N/A	99	84	62	40	98	83	−171
		Integral rel. to ERICA	N/A	2.0E−01	1.7E−01	5.0E−01	5.0E−01	5.6E−01	6.4E−01	1.0E+00
	Ext. dose	T(maximum) (d)	N/A	110	110	110	110	110	110	110
		Maximum (μGy h^{-1})	N/A	7.1E−01	7.4E−01	4.6E−01	3.1E+00	7.4E−01	1.4E+00	1.5E+00
		Half-time 80–110 d (d)	N/A	−209	−208	−208	−207	−209	−208	−209
		Integral rel. to ERICA	N/A	4.8E−01	5.0E−01	3.1E−01	2.1E+00	5.0E−01	9.7E−01	1.0E+00

[a] N/A values in Tables 4–8 signify no predictions for some models/radionuclides/organisms, or the unavailability parameters. No time of maximum in a monotonically increasing activity or dose curve is indicated as a maximum corresponding to $T = 110$ d. No half-time in a best-fit exponential function reflects insufficient statistical significance (as defined by a low coefficient of determination, r^2).

3.3. Macroalgae

Activity concentrations for macroalgae show similar features to those already discussed for benthic fish, with some differences due to the different $T_{B1/2}$s involved. Some specific instances are worth mentioning. For example, for ^{90}Sr, ^{131}I and ^{137}Cs, the BURN activity concentration prediction is quite close to the ERICA prediction, which is not surprising given that in this model the algae are not considered to be part of the food chain and the model uses the CR_{wo} approach, with a CR_{wo} from IAEA (2004). This explains the difference from the rest of dynamic models. For ^{90}Sr, ECOMOD follows the fluctuations in seawater activity concentration and gives higher results to BURN in absolute terms, likely due to the different way in which ECOMOD represents the uptake process. For ^{131}I, K-BIOTA gives significantly lower predictions than the rest of the models, linked to the way this model represents the macroalgae assuming a water uptake rate of 0.3 m^3 kg^{-1} d^{-1}. There is not enough information to fully explain this issue.

A similar behaviour to that for benthic fish is noted in that external dose rates increase with time so there is not a maximum (Table 7), and thus Table 7 reports 110 days as the time of maximum value for the period 80–110 d, and the half-time is negative. For benthic organisms, the external dose rate increases with time because it is dominated by the component for exposure to sediment, which increases as sediment activity concentrations gradually build-up. ^{131}I in ECOMOD also registers an increase by the end of the period (Fig. 5). In general, ECOMOD predictions tend to be at the higher end of the dynamic models group for the early period $T < 40$ days, whilst after that period they converge within the spread of the rest of the models; the effect being more pronounced for ^{137}Cs. For all models, the slope of the exponential attenuation region $T > 40$ d for ^{131}I is dominated by decay, as explained previously (this applies to all categories of biota).

The external dose rate predictions for BURN and ECOMOD form a distinct pattern in that such doses decrease mirroring the pattern of seawater activity concentrations (Fig. 5), albeit at different absolute scales. This is attributable to these models not using the external exposure pathway for sediment in dose calculations. The rest of the models form a consistent smooth pattern more akin to the time-series of sediment concentrations. In general, the grouping of the model predictions is similar to that for fish, with a tendency for tighter grouping in external dose.

3.4. Crustaceans and molluscs

For ^{90}Sr in crustaceans, ECOMOD gives different predictions from the rest of the dynamic models and more similar to the ERICA Tool prediction. This is because, in this model, the crustacean is assumed to have the same characteristics as zooplankton, which is modelled using a CR_{wo}, as in the ERICA Tool. For the period after 30 days, K-BIOTA records consistently the highest ^{90}Sr activity concentration and consequently internal dose, an order of magnitude above the average of all models. This can be tracked-back to the high ingestion rate multiplied by assimilation efficiency used for this model. For ^{131}I (also in crustaceans), BURN gives higher activity and internal dose predictions than the rest of the models (almost three orders of magnitude difference). This is because BURN-P considers crustaceans as detritus-feeders (and molluscs as filter-

Table 5
Activity concentration, internal and external dose rate for ^{90}Sr, ^{131}I and ^{137}Cs in pelagic fish: summary of indicator parameters.

Nuclide	Category	Parameter	BURN-P	ECOMOD	NRPA	IRSN	K-BIOTA	D-DAT	ANL	ERICA
^{90}Sr	Activity	T(maximum) (d)	N/A	40	43	35	46	41	29	26
		Maximum (Bq kg^{-1})	2.4E+02	3.4E+01	8.7E+02	6.3E+01	4.7E+03	5.3E+02	1.7E+02	2.0E+04
		Half-time 80–110 d (d)	−288	504	583	144	30	261	46	16
	Int. dose	T(maximum) (d)	110	40	43	35	46	41	29	26
		Maximum (μGy h^{-1})	1.5E−01	2.1E−02	5.4E−01	2.3E−02	2.9E+00	3.2E−01	1.1E−01	1.2E+01
		Half-time 80–110 d (d)	−288	505	583	144	30	261	46	16
		Integral rel. to ERICA	1.6E−01	2.5E−02	6.5E−01	2.5E−02	2.5E+00	3.7E−01	8.9E−02	1.0E+00
	Ext. dose	T(maximum) (d)	26	26	26	26	26	26	26	26
		Maximum (μGy h^{-1})	2.2E−02	2.2E−02	2.2E−02	1.7E−02	2.8E−02	4.0E−02	1.8E−02	2.2E−02
		Half-time 80–110 d (d)	16	16	16	16	16	16	16	16
		Integral rel. to ERICA	1.1E+00	1.0E+00	1.1E+00	7.6E−01	1.3E+00	2.0E+00	8.2E−01	1.0E+00
^{131}I	Activity	T(maximum) (d)	32	23	23	27	24	24	23	20
		Maximum (Bq kg^{-1})	3.6E+05	7.1E+03	1.5E+05	2.3E+04	1.2E+04	1.0E+04	5.7E+03	6.2E+04
		Half-time 80–110 d (d)	9	15	16	10	99	39	13	−142
	Int. dose	T(maximum) (d)	32	23	23	27	24	24	23	20
		Maximum (μGy h^{-1})	4.6E+01	9.2E−01	1.9E+01	2.0E+00	1.6E+00	1.4E+00	7.7E−01	8.1E+00
		Half-time 80–110 d (d)	9	15	16	10	100	39	13	−142
		Integral rel. to ERICA	1.8E+01	2.6E−01	5.3E+00	6.7E−01	3.6E−01	4.1E−01	2.3E−01	1.0E+00
	Ext. dose	T(maximum) (d)	20	20	20	20	20	20	20	20
		Maximum (μGy h^{-1})	1.4E+00	1.1E+01	1.4E+00	9.4E−01	1.4E+00	6.7E−01	1.4E+00	1.4E+00
		Half-time 80–110 d (d)	−141	−49	−141	−141	−142	−145	−141	−142
		Integral rel. to ERICA	1.0E+00	6.2E+00	1.0E+00	6.8E−01	1.0E+00	5.0E−01	9.8E−01	1.0E+00
^{137}Cs	Activity	T(maximum) (d)	51	36	37	35	49	37	36	27
		Maximum (Bq kg^{-1})	7.5E+03	5.8E+03	9.3E+03	2.1E+04	1.5E+04	1.4E+04	1.7E+04	1.5E+05
		Half-time 80–110 d (d)	194	82	72	53	32	71	70	12
	Int. dose	T(maximum) (d)	51	35	37	35	48	37	36	27
		Maximum (μGy h^{-1})	1.4E+00	1.0E+00	1.7E+00	2.5E+00	2.5E+00	2.5E+00	2.9E+00	2.6E+01
		Half-time 80–110 d (d)	194	82	72	53	32	71	70	12
		Integral rel. to ERICA	3.6E−01	2.5E−01	3.9E−01	5.3E−01	5.4E−01	5.7E−01	6.8E−01	1.0E+00
	Ext. dose	T(maximum) (d)	27	20	27	27	27	27	27	27
		Maximum (μGy h^{-1})	5.1E−01	3.6E+00	5.1E−01	3.2E−01	5.5E−01	2.5E−01	5.1E−01	5.1E−01
		Half-time 80–110 d (d)	12	27	12	12	12	12	12	12
		Integral rel. to ERICA	1.0E+00	6.0E+00	1.0E+00	6.3E−01	1.1E+00	5.1E−01	1.0E+00	1.0E+00

feeders) with a relatively high assimilation efficiency for radionuclides associated with particulate fractions potentially increasing the predictions by models that explicitly consider the ingestion pathway (Table 3). For ^{137}Cs in crustaceans, ECOMOD gives elevated predictions that follow the fast dynamic changes of concentration in seawater with a faster decreasing pattern than the other models. For external dose all the model predictions are similar. However for all radionuclides, BURN-P shows a markedly different decreasing pattern in the time-dependent internal dose prediction compared with the other dynamic models, mimicking the fluctuations of the radionuclide in seawater with the application of a constant CR, again because it does not include the sediment exposure component. The IRSN model also shows this behaviour for ^{90}Sr, attributable to fluctuations in the input data used for this study, which shows more clearly in some models than in others depending on the biological half-lives and other parameters used.

The same observations for crustacean apply almost identically to mollusc, with the exception that, for ^{90}Sr activity concentration and internal dose, the ECOMOD and the ERICA predictions are similar, whereas for mollusc the shape of the time-series activity concentration (and internal dose) is the same but ECOMOD's prediction is one order of magnitude below that of ERICA. The obvious explanation for this differential behaviour of ECOMOD is the concentration factor of 5×10^1 L kg^{-1} for crustacean (nearly identical to the ERICA CR_{wo} of 4.9×10^1 L kg^{-1}), whereas for mollusc ECOMOD uses a CR_{wo} of 1.2×10^1 L kg^{-1} compared with the ERICA value of 1.5×10^2 L kg^{-1}.

Tables 6 and 8 for crustaceans and molluscs give similar indicator parameters as the tables for the other organisms, with some negative half-times of attenuation in various categories of activity and dose for the post-acute period 80–110 days for ^{137}Cs (predicted activity concentration and all categories of dose). In this case the cause is not necessarily that the time series of data is monotonically increasing, but that it reflects fluctuations in the input modelling data in the chosen time period, whereas if one took the overall trend from 40 to 110 days it is generally decreasing, although not monotonically, hence the existence of a maximum value. ^{131}I in ECOMOD also registers a build-up attributable to the diffusive vertical transfer of ^{131}I to deeper water (Fig. 5). For all models except ECOMOD, the external dose rate for ^{137}Cs increases monotonically with time, also indicated by negative half-times in the post-acute period. For the molluscs the difference is that the BURN and ANL models register an attenuating profile of ^{90}Sr activity concentration and internal dose, and that the ^{131}I external dose rate is slightly decreasing.

Again, for crustacean and mollusc, the half-time of attenuation for ^{131}I is generally the shortest among all radionuclides, reflecting the fast decay of this radionuclide.

3.5. Comparison between dynamic models and the ERICA Tool

For benthic fish, Fig. 2 shows that the ERICA Tool prediction gives higher ^{90}Sr, ^{131}I and ^{137}Cs activity concentrations in the earlier part of the simulation ($T < 30$–40 d) and lower thereafter. This is a well-known issue with equilibrium models, which has been demonstrated previously (Vives i Batlle, 2014). It is caused by the fact that gradual uptake and turnover are not predicted by the CR-based models, which assume instantaneous equilibrium between radionuclide concentrations in biota and the surrounding medium. In the case of ^{131}I this is difficult to see because the mean of the dynamic models is distorted upwards by the relatively elevated prediction of the NRPA model, as explained previously (applies to both concentration and internal dose rates). Moreover, the dominant physical $T_{1/2}$ of 8 days tends to induce similar results. In

Table 6
Activity concentration, internal and external dose rate for ^{90}Sr, ^{131}I and ^{137}Cs in crustaceans: summary of indicator parameters.

Nuclide	Category	Parameter	BURN-P	ECOMOD	NRPA	IRSN	K-BIOTA	D-DAT	ANL	ERICA
^{90}Sr	Activity	T(maximum) (d)	42	26	N/A	27	43	27	34	26
		Maximum (Bq kg^{-1})	2.2E+02	4.0E+04	N/A	3.3E+02	2.8E+03	5.5E+03	2.2E+02	3.4E+04
		Half-time 80–110 d (d)	105	16	N/A	33	71	252	54	14
	Int. dose	T(maximum) (d)	42	26	N/A	27	43	27	34	26
		Maximum (μGy h^{-1})	1.4E−01	2.5E+01	N/A	1.2E−01	1.8E+00	3.5E+00	1.4E−01	2.2E+01
		Half-time 80–110 d (d)	105	16	N/A	33	72	252	54	14
		Integral rel. to ERICA	8.6E−02	1.2E+00	N/A	5.0E−02	1.1E+00	3.4E−01	6.9E−02	1.0E+00
	Ext. dose	T(maximum) (d)	26	26	N/A	26	26	26	26	26
		Maximum (μGy h^{-1})	1.6E−02	8.7E−03	N/A	1.1E−02	1.3E−02	9.2E−03	8.9E−03	9.2E−03
		Half-time 80–110 d (d)	14	148	N/A	18	266	209	210	209
		Integral rel. to ERICA	1.1E+00	7.7E−01	N/A	7.5E−01	1.8E+00	1.0E+00	9.6E−01	1.0E+00
^{131}I	Activity	T(maximum) (d)	31	20	N/A	35	29	28	34	26
		Maximum (Bq kg^{-1})	2.6E+05	6.9E+04	N/A	2.2E+02	2.2E+02	3.8E+02	5.2E+01	4.5E+03
		Half-time 80–110 d (d)	9	−142	N/A	9	14	54	8	30
	Int. dose	T(maximum) (d)	31	20	N/A	35	29	28	34	26
		Maximum (μGy h^{-1})	3.6E+01	9.7E+00	N/A	2.0E−02	3.0E−02	5.3E−02	7.1E−03	6.4E−01
		Half-time 80–110 d (d)	9	−142	N/A	9	14	54	8	30
		Integral rel. to ERICA	7.8E+01	6.6E+00	N/A	5.1E−02	5.7E−02	9.3E−02	1.6E−02	1.0E+00
	Ext. dose	T(maximum) (d)	26	27	N/A	27	37	27	27	27
		Maximum (μGy h^{-1})	2.2E−02	3.6E−02	N/A	2.4E−02	1.2E−01	3.0E−02	6.3E−02	6.1E−02
		Half-time 80–110 d (d)	30	10	N/A	10	10	10	10	10
		Integral rel. to ERICA	2.5E−01	5.6E−01	N/A	3.7E−01	1.9E+00	5.0E−01	1.0E+00	1.0E+00
^{137}Cs	Activity	T(maximum) (d)	49	27	N/A	60	65	52	52	34
		Maximum (Bq kg^{-1})	4.3E+03	8.8E+04	N/A	4.1E+02	8.1E+02	5.5E+02	5.2E+02	4.1E+02
		Half-time 80–110 d (d)	114	12	N/A	137	101	86	97	−171
	Int. dose	T(maximum) (d)	49	27	N/A	60	63	52	52	34
		Maximum (μGy h^{-1})	7.7E−01	1.6E+01	N/A	5.2E−02	1.5E−01	9.9E−02	9.1E−02	7.3E−02
		Half-time 80–110 d (d)	114	12	N/A	137	100	86	97	−171
		Integral rel. to ERICA	3.8E+01	1.2E+02	N/A	2.6E+00	6.9E+00	4.6E+00	4.4E+00	1.0E+00
	Ext. dose	T(maximum) (d)	34	110	N/A	110	110	110	110	110
		Maximum (μGy h^{-1})	2.2E−02	7.1E−01	N/A	3.7E−01	3.0E+00	7.1E−01	1.4E+00	1.4E+00
		Half-time 80–110 d (d)	−171	−209	N/A	−208	−208	−209	−208	−209
		Integral rel. to ERICA	4.7E−03	5.0E−01	N/A	2.6E−01	2.1E+00	5.0E−01	1.0E+00	1.0E+00

general, the ^{131}I results for ERICA are in the range of the dynamic predictions.

For pelagic fish, the mean of dynamic model predictions for ^{90}Sr is generally 2–3 orders of magnitude below the ERICA equilibrium prediction during the early accident phase. In contrast, for ^{137}Cs, similarly to the benthic fish case, ERICA predicts comparatively high activity concentrations at $T < 50$ d and lower at $T > 50$ d. Again, this behaviour is caused by the fact that gradual uptake and turnover are not predicted by the CR-based models, and the differences increase the shorter the $T_{B1/2}$ becomes. Since for pelagic fish $T_{B1/2}$s tend to be higher than for ^{131}I and the predictions appear to be more tightly grouped, it is natural that the effect is more pronounced for ^{137}Cs.

For the remaining species, the pattern is similar, depending on biological half-life for the organism and radionuclide in question, as well as by the occasional tendency of model predictions to be less tightly grouped. We observe that for ^{137}Cs in mollusc, the ERICA prediction appears to be somewhat lower than the mean of the dynamic models during the release phase after about >30 days. This result is a combination of various factors. One of the models (NRPA) actually uses the equilibrium CR_{wo} approach for mollusc, and some of the models calculate the activity in crustacean and mollusc by direct ingestion of organisms for which the equilibrium assumption is made.[3] For other models (e.g. D-DAT, ANL) the CR_{wo} determines the limit value that the activity concentration can reach and, as seen in Table 3, the ERICA CR_{wo} for mollusc (5.0×10^1 L kg^{-1}) (Copplestone et al., 2013), is somewhat lower than the CR_{wo}s used by the other models.

The half-times presented in Tables 4–8 for activity concentrations and internal dose rates from the predictions of the ERICA Tool are the same as those for the scenario water inputs, which is logical since the ERICA Tool calculates the activity concentration in biota by multiplication of the CR_{wo} by the activity concentration in the water.

Regarding external dose rates, for all organisms, ERICA gives similar results to the dynamic models. This was to be expected because there is 'nothing dynamic' in the calculation of the external dose rate and thus all the models approach the problem in the same way. Moreover, many of the models take the external DCC values from ERICA and the dosimetry components of the various models have previously been shown to give similar results (Vives i Batlle, 2011; Vives i Batlle et al., 2007a). For ^{131}I, decay is clearly the dominating influence at $T > 40$ d. In the case of pelagic fish, if one discounts the most notable high and low model predictions, the outputs for the ERICA Tool and the dynamic models are the closest together because external dose does not include the sediment pathway for organisms not living at the seabed, and thus possible sources of variability between models due to modelling dose from sediment are eliminated.

Although the models in this exercise did not use a correction for the degree of moisture assumed in sediment, it is worth mentioning in passing that this is another factor that may affect comparison between models. The ERICA Tool applies the DCCs to fresh mass activity concentrations, and allows a fixed percentage of moisture to be stated. Regarding the DCC variability induced by varying the degree of moisture in porous media with a water content varying from 0 (dry) to 100% (saturated), a previous study for soil suggest that, for a set of α, β, and γ emitters selected to cover

[3] The equilibrium assumption for 'simpler' organisms (those considered to have rapid uptake and short retention time of radioactivity) is made in three models, namely BURN (phytoplankton and macroalgae), K-BIOTA (phytoplankton) and NRPA (zooplankton and mollusc).

Table 7
Activity concentration and internal dose rate for ^{90}Sr, ^{131}I and ^{137}Cs in macroalgae: summary of indicator parameters.

Nuclide	Category	Parameter	BURN-P	ECOMOD	NRPA	IRSN	K-BIOTA	D-DAT	ANL	ERICA
^{90}Sr	Activity	T(maximum) (d)	26	26	N/A	27	34	28	27	26
		Maximum (Bq kg^{-1})	7.0E+03	2.0E+05	N/A	1.4E+03	9.3E+02	6.0E+03	5.8E+02	2.0E+04
		Half-time 80–110 d (d)	14	16	N/A	15	42	42	38	14
	Int. dose	T(maximum) (d)	26	26	N/A	27	28	28	27	26
		Maximum (μGy h^{-1})	3.3E+00	9.1E+01	N/A	4.4E−01	3.3E−01	2.7E+00	2.8E−01	9.2E+00
		Half-time 80–110 d (d)	14	16	N/A	15	42	42	38	14
		Integral rel. to ERICA	3.8E−01	1.0E+01	N/A	2.4E−01	3.6E−01	1.8E+00	3.0E−01	1.0E+00
	Ext. dose	T(maximum) (d)	26	26	N/A	26	26	26	26	26
		Maximum (μGy h^{-1})	1.3E−01	1.6E−01	N/A	1.2E−01	1.4E−01	8.0E−02	6.8E−02	8.0E−02
		Half-time 80–110 d (d)	14	16	N/A	47	266	209	210	209
		Integral rel. to ERICA	1.1E+00	1.3E+00	N/A	9.8E−01	2.2E+00	1.0E+00	8.4E−01	1.0E+00
^{131}I	Activity	T(maximum) (d)	26	20	N/A	35	29	29	29	26
		Maximum (Bq kg^{-1})	1.2E+06	6.9E+06	N/A	7.4E+05	1.2E+02	3.8E+05	6.3E+05	4.9E+05
		Half-time 80–110 d (d)	30	−142	N/A	9	13	31	14	30
	Int. dose	T(maximum) (d)	26	20	N/A	35	29	29	29	26
		Maximum (μGy h^{-1})	1.3E+02	6.9E+02	N/A	5.9E+01	1.2E−02	3.8E+01	7.0E+01	4.9E+01
		Half-time 80–110 d (d)	30	−142	N/A	9	13	31	14	30
		Integral rel. to ERICA	2.6E+00	6.2E+00	N/A	1.9E+00	3.2E−04	9.9E−01	1.8E+00	1.0E+00
	Ext. dose	T(maximum) (d)	26	20	N/A	27	37	27	27	27
		Maximum (μGy h^{-1})	2.6E−02	1.6E+00	N/A	2.4E−02	1.4E−01	3.7E−02	7.1E−02	7.4E−02
		Half-time 80–110 d (d)	30	−141	N/A	10	10	10	10	10
		Integral rel. to ERICA	2.4E−01	6.6E+00	N/A	3.1E−01	1.9E+00	5.0E−01	9.6E−01	1.0E+00
^{137}Cs	Activity	T(maximum) (d)	34	27	N/A	49	49	51	50	34
		Maximum (Bq kg^{-1})	3.8E+03	8.8E+04	N/A	8.6E+02	3.0E+02	1.7E+03	6.8E+02	7.4E+03
		Half-time 80–110 d (d)	−171	12	N/A	50	50	80	68	−171
	Int. dose	T(maximum) (d)	34	27	N/A	49	48	51	50	34
		Maximum (μGy h^{-1})	5.4E−01	1.1E+01	N/A	8.8E−02	3.7E−02	2.2E−01	9.2E−02	9.6E−01
		Half-time 80–110 d (d)	−171	12	N/A	50	50	80	68	−171
		Integral rel. to ERICA	5.6E−01	6.4E+00	N/A	2.8E−01	1.2E−01	7.7E−01	3.2E−01	1.0E+00
	Ext. dose	T(maximum) (d)	34	27	N/A	110	110	110	110	110
		Maximum (μGy h^{-1})	2.5E−02	6.0E−01	N/A	4.2E−01	3.6E+00	8.3E−01	1.6E+00	1.7E+00
		Half-time 80–110 d (d)	−171	12	N/A	−208	−207	−209	−208	−209
		Integral rel. to ERICA	4.6E−03	5.8E−02	N/A	2.5E−01	2.1E+00	5.0E−01	9.8E−01	1.0E+00

the range of possible emission energies, the corresponding DCCs are within a factor of 3 at maximum (Beaugelin-Seiller, 2016).

The dynamic models (when not using a CR_{wo} approach) predict the time of peak of activity concentrations in the biota with a delay compared to the equilibrium approach, due to the ability to predict gradual build-up of the radionuclide instead of assuming instantaneous equilibration. Taking the example of ^{90}Sr in benthic fish (roughly comparable to the other organisms), all models predict the maximum activity concentration at around 40 ± 5 d,[4] a 14-day 'delay' compared with ERICA. For ^{131}I and ^{137}Cs, the dynamic models predict a maximum at 34 ± 2 and 53 ± 4 days, respectively, which is 7 and 19 days later than ERICA, respectively. The differences between radionuclides reflect differences in biological half-life and decay for the different radionuclides.

For pelagic fish, similar shifting of the maximum peak of activity for the dynamic models compared with the ERICA Tool is observed: the maximum is situated at 39 ± 6, 25 ± 3 and 40 ± 7 d for ^{90}Sr, ^{131}I and ^{137}Cs, which is somewhat lower than, but reasonably close to, the values for benthic fish. Comparing with 26, 20 and 27 days for ERICA, this gives 'delay' times of 13, 5 and 13 days, which is similar to the 14, 8 and 19 days calculated for benthic fish.

For macroalgae, the delay times for ^{90}Sr, ^{131}I and ^{137}Cs activity concentration can also be calculated as the dynamic model average times at the time of maximum activity concentration of 28 ± 3, 28 ± 5 and 45 ± 10, minus the ERICA equivalents of 26, 26 and 34 days, respectively, giving delay times of 2, 2 and 11 days. The lower delay times compared with fish are due to different assumed dynamics of uptake by macroalgae. What is seen here probably reflects the higher affinity of fish for retaining Sr, which as analogue of Ca accumulates in the skeleton, and I to a lesser degree.

For the crustaceans, the delay times for ^{90}Sr, ^{131}I and ^{137}Cs activity concentration are the dynamic model average time at maximum of 33 ± 8, 30 ± 5 and 51 ± 13 minus the ERICA equivalents of 26, 26 and 34 days, respectively, giving delay times of 7, 4 and 17 days. For molluscs, the delay times are 30 ± 4, 30 ± 6 and 44 ± 11 minus 26, 26 and 34 days, giving 4, 4 and 10 days.

There is therefore no obvious difference between macroalgae, crustaceans and molluscs, and again ^{137}Cs records the longest delay time for these organisms.

As a caveat, the above comparison of 'delay time' between the ERICA Tool and the mean of the dynamic models is only qualitative because, when taking into account the statistics, ERICA appears to be in the range of the other models.

4. Discussion

This intercomparison involved four different types of models: (a) models based on first-order kinetics of radionuclide exchange between the organism and the water (i.e. ANL, D-DAT, IRSN); (b) models that additionally model ingestion as a separate mechanism using ingestion rates and absorption efficiencies (i.e. NRPA, BURN and K-BIOTA); (c) a model that include metabolism and as a consequence can represent variable biomass (i.e. ECOMOD) and (d) an equilibrium model using CR_{wo} values (i.e. the ERICA Tool). It is therefore not surprising that the dynamic models give a range of results which in many cases we have been able to explain as due to differences in parameterisation or on the mathematical approach used by these models.

4.1. Overall features of the intercomparison

Overall, the intercomparison gives logical resultsIn general,

[4] Uncertainties in this section are quoted at the level of ±1 standard deviation (1σ).

Table 8
Activity concentration, internal and external dose rate for ^{90}Sr, ^{131}I and ^{137}Cs in mollusc: summary of indicator parameters.

Nuclide	Category	Parameter	BURN-P	ECOMOD	NRPA	IRSN	K-BIOTA	D-DAT	ANL	ERICA
^{90}Sr	Activity	T(maximum) (d)	34	26	N/A	27	35	28	27	26
		Maximum (Bq kg^{-1})	7.8E+02	9.7E+03	N/A	6.6E+02	3.8E+03	8.3E+03	1.5E+03	1.1E+05
		Half-time 80–110 d (d)	52	16	N/A	33	29	55	14	14
	Int. dose	T(maximum) (d)	34	26	N/A	27	35	28	27	26
		Maximum (μGy h^{-1})	4.5E−01	5.6E+00	N/A	2.3E−01	2.2E+00	4.8E+00	9.0E−01	6.1E+01
		Half-time 80–110 d (d)	52	16	N/A	33	29	55	14	14
		Integral rel. to ERICA	8.4E−02	9.5E−02	N/A	3.4E−02	3.0E−01	8.2E−01	6.8E−02	1.0E+00
	Ext. dose	T(maximum) (d)	26	26	N/A	26	26	26	26	26
		Maximum (μGy h^{-1})	5.4E−02	2.9E−02	N/A	3.4E−02	4.0E−02	3.1E−02	2.7E−02	3.1E−02
		Half-time 80–110 d (d)	14	148	N/A	21	269	209	210	209
		Integral rel. to ERICA	1.1E+00	7.7E−01	N/A	6.9E−01	1.7E+00	1.0E+00	8.8E−01	1.0E+00
^{131}I	Activity	T(maximum) (d)	27	20	N/A	35	29	35	34	26
		Maximum (Bq kg^{-1})	9.4E+05	6.9E+04	N/A	7.4E+02	4.1E+02	1.1E+03	1.3E+02	1.0E+06
		Half-time 80–110 d (d)	10	−142	N/A	9	14	11	8	30
	Int. dose	T(maximum) (d)	27	20	N/A	35	29	35	34	26
		Maximum (μGy h^{-1})	1.1E+02	8.3E+00	N/A	5.4E−02	4.6E−02	1.3E−01	1.5E−02	1.2E+02
		Half-time 80–110 d (d)	10	−143	N/A	9	14	11	8	30
		Integral rel. to ERICA	1.1E+00	3.0E−02	N/A	6.9E−04	4.6E−04	1.6E−03	1.8E−04	1.0E+00
	Ext. dose	T(maximum) (d)	26	27	N/A	27	37	27	27	27
		Maximum (μGy h^{-1})	2.4E−02	4.0E−02	N/A	2.3E−02	1.3E−01	3.4E−02	6.9E−02	6.8E−02
		Half-time 80–110 d (d)	30	10	N/A	10	10	10	10	10
		Integral rel. to ERICA	2.5E−01	5.6E−01	N/A	3.1E−01	1.9E+00	5.0E−01	1.0E+00	1.0E+00
^{137}Cs	Activity	T(maximum) (d)	39	27	N/A	60	49	45	44	34
		Maximum (Bq kg^{-1})	1.0E+04	1.1E+05	N/A	5.0E+02	9.7E+02	2.0E+03	1.8E+03	3.8E+03
		Half-time 80–110 d (d)	54	12	N/A	137	35	28	24	−171
	Int. dose	T(maximum) (d)	39	27	N/A	60	48	45	44	34
		Maximum (μGy h^{-1})	1.6E+00	1.6E+01	N/A	4.9E−02	1.5E−01	3.0E−01	2.6E−01	5.8E−01
		Half-time 80–110 d (d)	54	12	N/A	137	35	28	24	−171
		Integral rel. to ERICA	8.7E+00	1.5E+01	N/A	3.1E−01	7.1E−01	1.3E+00	1.1E+00	1.0E+00
	Ext. dose	T(maximum) (d)	34	110	N/A	110	110	110	110	110
		Maximum (μGy h^{-1})	2.5E−02	7.9E−01	N/A	3.6E−01	3.3E+00	7.9E−01	1.6E+00	1.6E+00
		Half-time 80–110 d (d)	−171	−209	N/A	−208	−210	−209	−208	−209
		Integral rel. to ERICA	4.7E−03	5.0E−01	N/A	2.3E−01	2.1E+00	5.0E−01	9.9E−01	1.0E+00

activity and internal dose predictions by each model do not show significant differences in terms of their time evolution. ECOMOD and BURN have methodological similarities and, not surprisingly, sometimes form a distinct data group compared with the rest. The ERICA equilibrium approach gives higher predictions in the acute (uptake-driven) phase and lower in the chronic phase compared to the dynamic predictions where turnover dominates.

As the $T_{B1/2}$ increases, the activity in biota and thus internal dose predictions from the dynamic model in the early phase (where they themselves do not use a CR_{wo} approach) are progressively lower than predicted by the equilibrium model. In relative terms, the dispersion between the results from different models increases in order generally coinciding with decreasing order of biological half-life. The NRPA and BURN models give somewhat higher answers than the other models due to a combination of ingestion rate, absorption efficiency and the introduction of conservatism at the lowest trophic level where a CR_{wo} approach is used.

The sediment activity concentration values used in this exercise were an input they were not calculated by the models. If this had not been the case, there would be an additional layer of conservatism involved in calculating external doses to benthic organisms using activity concentrations in sediment derived from water concentrations. Estimations using the D-DAT show that the estimated ^{137}Cs sediment concentration can be a factor of ~ 20 lower when using a dynamic sediment model compared with the equilibrium K_d assumption, and external dose rates to benthic organisms vary by the same factor (Vives i Batlle, 2016). An equilibrium K_d model could be far from conservative, however, once water concentrations decline and the radioactivity retained by the sediment becomes the dominant source term (depending on the conditions under which the k_d was originally modelled).

4.2. Integrated doses

The integrated doses (internal and external) were calculated over the period 0–40 days, a time interval arbitrarily chosen to reflect the acute phase of the accident. The results show common features when expressed as a ratio of the integrated magnitude averaged for the dynamic models and that for ERICA (even though some of the dynamic models deviate as much/more than ERICA).

For internal dose, this ratio tends to be below unity for ^{90}Sr and ^{131}I, signifying that for the uptake phase the biota is accumulating dynamically below the steady state limit (the 40-day period includes the initial part of the release where the dynamic models predict concentration in biota below the equilibrium level in respect of the environmental concentration due to retention, but for the majority of the 40-day period it is the uptake phase that dominates). However, the ratio is significantly higher in some instances, and more notably for ^{137}Cs in macroalgae, mollusc and crustacean in most of the models. This is because, in reality, some dynamic model predictions exceed the ERICA Tool (which ran with the most up-to-date CR_{wo} compilation at the time of the assessment, using data from Copplestone et al. (2013)) and the mean of the dynamic models is distorted upwards by relatively elevated ECOMOD predictions.

Although the internal dose rate prediction of a dynamic model is generally very different from that of an equilibrium model, the difference is not so pronounced for the integrated dose over the whole history of the accident (all other factors like DCC_{int}, CR_{wo}, etc. being the same). This is evidenced by calculating the mean value of the integral relative to the ERICA Tool for the dynamic models, using data from Tables 4–8. This mean value is lower by less than a factor of three for all organism groups. In practice, the relative low prediction of the dynamic models compared with ERICA in the

early phase is being partially compensated by the inverse phenomenon during the period when water concentrations are decreasing. This can be illustrated by a theoretical example, as seen below.

In the extreme limit case in which, due to an accidental discharge, the activity concentration in seawater reaches abruptly an elevated level and, after a transient time period τ, it returns rapidly to its previous low level, the total dose (integrated between t = 0 and infinity) as predicted by both equilibrium and dynamic models would be identical. This can be demonstrated mathematically using the D-DAT governing equation, simplified for the case $A_w = const.$ ($V >> M$) and further assuming (for simplicity) that the decay constant is 0: $\frac{dA_O}{dt} = -k_O\left(A_O - \frac{k_W A_W}{k_O}\frac{V}{M}\right)$. Hence, for the uptake ($t = 0$ to $t = \tau$) we have $A_O(t) = \frac{k_W A_W}{k_O}\frac{V}{M}(1 - e^{-k_O t}) = CR \times A_W(1 - e^{-k_O t})$ and for the release phase where $t > \tau$ with $K_w = 0$, $A_0(t) = CR \times A_W(1 - e^{-k_O \tau})e^{-k_0(t-\tau)}$ where $k_O = \frac{\ln 2}{T_{B1/2}}$. The total integrated internal dose over the full period ($t = 0$ to $t = \infty$) D_0 is the integration of the sum of the uptake and release functions, hence $D_O = CR \times A_W \times \tau \times DCC_{int}$. By implication, in a situation like this, the equilibrium approach would give a similar estimate of risk (relating to a hypothetical benchmark for acute exposure expressed in terms of total dose rather than dose rate), compared with the dynamic approach for such a scenario.

However, the above idealised case is not the same as the present study, due to the fact that there was a complex pulsed pattern of discharges. In addition, in practice, integration of the dose rate is not performed to time equalling infinity, but over a defined period, as a consequence of which the ratio of D_0 to the ERICA integrated dose $D_O = CR \times A_W \times \tau \times DCC_{int}$ is less than unity.

4.3. Measures of dispersion

In order to further explore the differences in predictions between the ERICA Tool and the dynamic models (considered as a group) in a simple way, we introduced three magnitudes: the magnitude ratio (*MR*), the mean relative standard deviation (*MSTD*) and the 'dispersion to difference ratio' (*DDR*), defined as follows:

$$MR = \sqrt{\frac{1}{N}\sum_{i=1}^{N}\left(\frac{E_i}{\mu_i}\right)^2} \quad MSTD = \sqrt{\frac{1}{N}\sum_{i=1}^{N}\left(\frac{\sigma_i}{\mu_i}\right)^2}$$

$$DDR = \sqrt{\frac{1}{N}\sum_{i=1}^{N}\left(\frac{\sigma_i}{\mu_i - E_i}\right)^2}$$

where E_i is the prediction of the 'reference' model (the ERICA Tool), and σ_i and μ_i are the standard deviation and the arithmetic mean of the outputs of the seven dynamic models at a point in time t_i. The *MR* quantifies how intrinsically different is the mean of the dynamic modelling predictions to the ERICA Tool in absolute terms. The higher the *MR*, the more the ERICA Tool gives high predictions in comparison with the dynamic models considered as a set (and when the mean of the dynamic models equals the ERICA prediction, MR = 1). The *MSTD* illustrates how tightly bound together the model predictions are packed around each other relative the mean of the results. The *DDR* gives information on the relative scale of the statistical spread between the dynamic model predictions, and the distance between the mean of the dynamic model predictions and the equilibrium prediction by the ERICA Tool. If *DDR* <<1 the dynamic model outputs group together at a distance from the prediction of the equilibrium model. If $DDR \geq 1$, it is possible to say that if there is any difference in prediction between ERICA and the set of dynamic models, then it is masked by the statistical dispersion of the dynamic predictions.

The *MR*, *MSTD* and *DDR* results for all organisms and radionuclides are given in Table 9. *MRs* for activity & internal dose are in the range 0.02–15. Significantly higher predictions of some dynamic models compared with the closer predictions of a main group result in elevated μ_i in several cases reflected in MR lower than 1; for example, we have explained how the BURN-POSEIDON and ECOMOD predictions for macroalgae, crustacean and mollusc raise the average of the dynamic models significantly, masking the tendency of the remaining dynamic models to generally predict significantly different results from the ERICA Tool. The data are evenly distributed above and below 1, but an overall average MR of 4 for all radionuclides, biota and non-external dose categories can be derived.

For ^{90}Sr the highest *MR* values for activity concentration and internal dose rate are in the order pelagic fish > mollusc > benthic fish > crustacean > macroalgae. For ^{137}Cs the ordering is pelagic fish > benthic fish > macroalgae > mollusc > crustacean. For ^{131}I the order is mollusc > benthic fish > pelagic fish > macroalgae > crustacean. This roughly reflects the general tendency for organisms with a longer biological half-life to be associated with a higher prediction by the ERICA Tool when compared with the dynamic models over the first 40 d of the assessment period, although the effect is masked by the fact that not all the models used the same biological half-lives or even the same $T_{B1/2}$-based calculation approach, and that some dynamic models use a CR_{wo} approach for 'simple' organisms.

The *MSTD* calculation demonstrates the variability of dynamic modelling results with values in the range 0.6–40 (for activity and internal dose), indicating a substantial spread of the models, especially for ^{131}I, though in several cases one or two models are responsible for the widening of the range. The *DDR* values for ^{137}Cs are generally above unity. Benthic fish record the lowest *DDRs* for all radionuclides.

Table 9
Mean scale ratio (MR), mean relative standard deviation between dynamic model predictions (MSTD) and figure of merit (DDR) for dynamic modelling compared with ERICA predictions.

Species	Nuclide	Category	MR	MSTD	DDR
Benthic fish	^{90}Sr	Activity concentration	7.9E+00	1.4E+00	1.6E+00
		Internal dose rate	7.9E+00	1.4E+00	1.6E+00
	^{131}I	Activity concentration	6.4E−01	2.1E+00	5.0E+00
		Internal dose rate	6.5E−01	2.1E+00	5.6E+00
	^{137}Cs	Activity concentration	1.2E+01	1.0E+00	6.9E−01
		Internal dose rate	1.3E+01	1.0E+00	6.8E−01
Pelagic fish	^{90}Sr	Activity concentration	9.4E+00	1.4E+00	1.9E+00
		Internal dose rate	9.5E+00	1.5E+00	1.9E+00
	^{131}I	Activity concentration	5.0E−01	1.5E+00	1.5E+01
		Internal dose rate	5.1E−01	1.6E+00	3.1E+01
	^{137}Cs	Activity concentration	1.3E+01	8.3E−01	1.1E+00
		Internal dose rate	1.5E+01	7.1E−01	1.6E+00
Crustacean	^{90}Sr	Activity concentration	2.6E+00	1.8E+00	3.2E+00
		Internal dose rate	2.6E+00	1.8E+00	3.8E+00
	^{131}I	Activity concentration	7.3E−02	2.0E+00	2.9E+00
		Internal dose rate	7.3E−02	2.0E+00	2.9E+00
	^{137}Cs	Activity concentration	1.7E−02	2.3E+00	2.4E+00
		Internal dose rate	1.7E−02	2.3E+00	2.4E+00
Macroalgae	^{90}Sr	Activity concentration	4.2E−01	1.9E+00	3.6E+00
		Internal dose rate	4.3E−01	1.9E+00	3.6E+00
	^{131}I	Activity concentration	2.5E−01	1.4E+00	3.5E+01
		Internal dose rate	2.5E−01	1.4E+00	5.4E+00
	^{137}Cs	Activity concentration	2.9E−01	2.2E+00	1.5E+01
		Internal dose rate	2.9E−01	2.2E+00	1.3E+01
Mollusc	^{90}Sr	Activity concentration	8.3E+00	1.4E+00	7.4E+00
		Internal dose rate	8.5E+00	1.5E+00	4.1E+01
	^{131}I	Activity concentration	4.7E+00	2.3E+00	1.2E+01
		Internal dose rate	4.7E+00	2.3E+00	1.2E+01
	^{137}Cs	Activity concentration	1.2E−01	2.1E+00	4.7E+00
		Internal dose rate	1.2E−01	2.1E+00	4.7E+00

4.4. Perspectives for future work

After performing this exercise and noticing significant variability between dynamic models, we recommend that the individual models should be further validated by comparing model predictions to actual data. The ideal test is a single short pulse rather than fluctuating concentrations, because the spectrum of fluctuations may distract from resolution of the time-response of the system receiving the input. Optimisation of model biokinetic parameters in such a test would result in more refined model predictions and greater convergence of the models. The $T_{B1/2}$ database for terrestrial and aquatic wildlife developed under the recent IAEA MODARIA would be useful in this respect (Beresford et al., 2015a, 2015b), as would compiling a database of ingestion rates and assimilation efficiencies for marine biota. Linked to this is a need to develop allometric methods to cover data gaps in transfer parameters and biological half-lives (Beresford et al., 2016).

The second important issue concerning the application of dynamic models to accidental situations in the marine environment is to introduce the representation of the dynamic transfer between seawater and sediments, thus improving external dose calculations for benthic organisms. Some of the models considered have now the ability to do this (Vives i Batlle, 2016).

A major issue for the future is how to explain the sustained radionuclide concentrations in fish from the vicinity of Fukushima up to the present time (Johansen et al., 2015) with particular emphasis on the incorporation of radionuclides from sediments to benthic foodwebs including to higher trophic levels. Most models studied here do not have this capability, but some, such as the NRPA approach and K-BIOTA are developing in that direction. Having compared and tested a number of 'first-generation' dynamic models, attention should turn to developing a 'second generation' of models incorporating marine foodchain representation (and to ultimately couple biological transfer models with ocean transport and dispersion models). In fact, the scope for this new generation of models is clearly wider than issues related to radionuclide transport and suggests an agenda in which radionuclide transport models are integrated with models for nutrient transport and the transport of other non-radioactive pollutants. However, such models would require values for substantial numbers of parameters, and an 'obvious' alternative to try first would be to obtain more appropriate CR_{wo}s for use in existing 'first generation' dynamic models.

Since most dynamic transfer models still use CR_{wo}'s implicitly (Brown et al., 2004; EPIC, 2003; Fievet and Plet, 2003; Heling and Bezhenar, 2009; Lepicard et al., 2004; Rowan and Rasmussen, 1996; Vives i Batlle et al., 2008), they are still susceptible to some of the drawbacks of these parameters. Even foodchain models are subject to this, as they generally use CR_{wo} at lower trophic levels. The only way around these problems is to use fully process based models, though the risk of developing relatively highly parameterised models limits the effectiveness of the end product. In general, we always advise keeping models as simple as possible.

This study has illustrated the shortcomings of equilibrium models in non-equilibrium conditions. In the case of the Fukushima accident it is probably true to say that the application of an equilibrium model at the early stages of an accident (e.g. Garnier-Laplace et al., 2011) is likely to overestimate the risk to biota. For planned authorised discharges involving continuous releases or gradual changes in discharge concentrations, if the timeframe of interest is long (e.g. years or decades) the equilibrium modelling approach is justified. For emergency or intermittent release scenarios involving abrupt changes in discharge concentrations, if the timeframe of the assessment is short (hours to a few months), then dynamic models of radionuclide transfer to biota are required. This is especially true for organisms that respond slowly to a change in ambient radioactivity concentration. On the other hand, there comes a time post-accident at which, for practical purposes, equilibrium modelling also suffices. A simulation carried-out with the D-DAT model suggests that this period is of the order of hundreds of days.

5. Conclusions

An intercomparison of models able to calculate dynamically transfer of radionuclides to biota and subsequent dose rates, has been performed in the context of a model-simulated scenario based on the Fukushima accident. The results must not be viewed as a radiological assessment, but should be regarded as purely a model intercomparison. This is because the study was performed at a single location, whereas a radiological impact assessment would require spatially distributed data. Additionally, the study uses inputs modelled by different codes instead of measured water and sediment data, adding an additional layer of uncertainty to the exercise. Radiological assessments of the Fukushima marine environment can be found in UNSCEAR (2014) and IAEA (2015). The work conducted here in no way suggests issues with these assessments, though as noted above, activity concentrations in, especially, benthic fish are remaining higher than initially anticipated (Johansen et al., 2015).

The intercomparison shows a shifting of the maximum peak of activity for the different dynamic models compared with an equilibrium transfer model, as the dynamic models include consideration of the retention of radionuclides by biota following reductions in environmental concentrations. The exponential rate of loss estimated by the models past the discharge peak is slower than expected if depuration $T_{B1/2}$ was the only operating process, reflecting the rate of predicted decline in ambient seawater concentrations.

The differences between the ERICA Tool and the dynamic models increase with $T_{B1/2}$. The time-integrated doses over days 0–40 after the accident calculated by the dynamic models are generally similar to those obtained using the ERICA Tool, because the lower prediction of the dynamic models in the predominantly uptake phase is partially offset by higher prediction in the release phase.

A tendency of the dynamic models to predict lower activities/internal doses than the ERICA Tool in the early phase of the accident is observable from Figs. 2–6. However, our statistical analysis shows that this trend is partially masked by the statistical spread of the model predictions, due to model variability. However, it is a well-known mathematical result that the CR_{wo} approach leads to an instantaneous fall in activity concentrations in direct correlation with declining seawater levels, whereas the biokinetic models more correctly assume a substantial retention with relatively slow depuration determined by the biological half-life. This effect has been seen more clearly when using some of the models in isolation (e.g. D-DAT, ECOMOD and NRPA model) (Psaltaki et al., 2013; Vives i Batlle, 2016; Vives i Batlle et al., 2014).

We have highlighted the need to examine the reasons for the differences in predictions made using different dynamic models and the need to refine their structure and parameterisation. Such refinement would result in more consistent model predictions. In particular, we note the need to determine more accurately the biokinetic model parameters, signalling the direction for future investigations.

Acknowledgements

This paper is dedicated to the memory of our friend and colleague Rudie Heling, who encouraged this work to be conducted.

This work was conducted in the frame of the IAEA Modelling and Data for Radiological Impact Assessments (MODARIA) programme (http://www-ns.iaea.org/projects/modaria/default.asp?l=116#3), by Working Group 8 (Biota modelling: Further development of transfer and exposure models and application to scenarios) and in collaboration with Working Group 10 (Modelling of marine dispersion and transfer of radionuclides accidentally released from land-based facilities).

References

Beaugelin-Seiller, K., 2016. Effects of soil water content on the external exposure of fauna to radioactive isotopes. J. Environ. Radioact. 151 (1), 204–208.

Beaugelin-Seiller, K., Jasserand, F., Garnier-Laplace, J., Gariel, J.C., 2006. Modeling radiological dose in non-human species: principles, computerization, and application. Health Phys. 90 (5), 485–493.

Beresford, N.A., Barnett, C.L., Brown, J., Cheng, J.J., Copplestone, D., Filistovic, V., Hosseini, A., Howard, B.J., Jones, S.R., Kamboj, S., Kryshev, A., Nedveckaite, T., Olyslaegers, G., Saxén, R., Sazykina, T., Vives i Batlle, J., Vives-Lynch, S., Yankovich, T., Yu, C., 2008. Inter-comparison of models to estimate radionuclide activity concentrations in non-human biota. Radiat. Environ. Biophys. 47 (4), 491–514.

Beresford, N.A., Beaugelin-Seiller, K., Burgos, J.,M.,C., Fesenko, S., Kryshev, A., Pachal, N., Real, A., Su, B.S., Tagami, K., Vives i Batlle, J., Vives-Lynch, S., Wells, C., Wood, M.D., 2015a. Radionuclide biological half-life values for terrestrial and aquatic wildlife. J. Environ. Radioact. 150, 270–276.

Beresford, N.A., Beaugelin-Seiller, K., Wells, C.V.-L.,S., Vives i Batlle, J., Wood, M.D., Tagami, K., Real, A., Burgos, J., Fesenko, S., Cujic, M., Kryshev, A., Pachal, N., Su, B.S., Barnett, C.L., Uchida, S., Hinton, T., Mihalík, J., Stark, K., Willrodt, C., Chaplow, J.S., 2015b. A Database of Radionuclide Biological Half-life Values for Wildlife. NERC-Environmental Information Data Centre. http://dx.doi.org/10.5285/b95c2ea7-47d2-4816-b942-68779c59bc4d.

Beresford, N.A., Wood, M.D., Vives i Batlle, J., Yankovich, T.L., Bradshaw, C., Willey, N., 2016. Making the most of what we have: application of extrapolation approaches in radioecological wildlife transfer models. J. Environ. Radioact. 151 (2), 373–386.

Brown, J., Børretzen, P., Dowdall, M., Sazykina, T., Kryshev, I., 2004. The derivation of transfer parameters in the assessment of radiological impacts to Arctic Marine Biota. Arctic 57 (3), 279–289.

Brown, J.E., Alfonso, B., Avila, R., Beresford, N.A., Copplestone, D., Pröhl, G., Ulanovsky, A., 2008. The ERICA tool. J. Environ. Radioact. 99 (9), 1371–1383.

Citra, M.J., 1997. Modelmaker 3.0 for Windows. J. Chem. Inf. Comput. Sci. 37 (6), 1198–1200.

Copplestone, D., Beresford, N.A., Brown, J.E., Yankovich, T., 2013. An international database of radionuclide concentration ratios for wildlife: development and uses. J. Environ. Radioact. 126, 288–298.

EPIC, 2003. The "EPIC" impact assessment framework. Towards the protection of the Arctic environment from the effects of ionising radiation. In: Brown, J., Thorring, H., Hosseini, A. (Eds.), EPIC (Environmental Protection from Ionising Contaminants) Report ICA2-CT-2000-10032, Østerås, Norway, p. 175. http://www.erica-project.org/.

Fievet, B., Plet, D., 2003. Estimating biological half-lifes of radionuclides in marine compartments from environmental time-series measurements. J. Environ. Radioact. 65 (1), 91–107.

Fiévet, B., Voiseux, C., Rozet, M., Masson, M., Bailly du Bois, P., 2006. Transfer of radiocarbon liquid releases from the AREVA La Hague spent fuel reprocessing plant in the English channel. J. Environ. Radioact. 90 (3), 173–196.

Fisher, N.S., 2002. Advantages and problems in the application of radiotracers for determining bioaccumulation of contaminants in aquatic organisms. In: Børretzen, P., Jølle, T., Strand, P. (Eds.), Proceedings of the International Conference on Radioactivity in the Environment. 1–5 September 2002. Norwegian Radiation Protection Authority, Monaco. Østerås, Norway, pp. 573–576.

Garnier-Laplace, J., Beaugelin-Seiller, K., Hinton, T.G., 2011. Fukushima wildlife dose reconstruction signals ecological consequences. Environ. Sci. Technol. 45, 5077–5078.

Gear, C.W., 1971. Numerical Initial Value Problems in Ordinary Differential Equations. Prentice-Hall, NJ.

Heling, R., Bezhenar, R., 2009. Modification of the dynamic radionuclide uptake model BURN by salinity driven transfer parameters for the marine foodweb and its integration in POSEIDON-R. Radioprotection 44 (5), 741–746.

Heling, R., Koziy, L., Bulgakov, V., 2002. On the dynamical uptake model developed for the uptake of radionuclides in marine organisms for the POSEIDON-R model system. Radioprotection 37 (C1), 833–838.

IAEA, 2004. Sediment Distribution Coefficients and Concentration Factors for Biota in the Marine Environment. Technical Reports Series No. 422. International Atomic Energy Agency, Vienna.

IAEA, 2014. Handbook of Parameter Values for the Prediction of Radionuclide Transfer to Wildlife. International Atomic Energy Agency Technical Report Series 479, p. 211. Vienna.

IAEA, 2015. The Fukushima Daiichi Accident. STI/PUB/1710. International Atomic Energy Agency, Vienna, p. 1254.

ICRP, 2008. Environmental Protection: the Concept and use for Reference Animals and Plants.International Commission on Radiological Protection Publication 108. Annals of the ICRP 38 (4-6), 76. Elsevier Ltd.

ICRP, 2009. Transfer parameters for reference animals and plants. International Commission on Radiological protection. Environmental protection publication 114. Ann. ICRP 39 (6) (Elsevier, Oxford).

Johansen, M.P., Ruedig, E., Tagami, K., Uchida, S., Higley, K., Beresford, N.A., 2015. Radiological dose rates to marine fish from the Fukushima Daiichi accident: the first three years across the North Pacific. Environ. Sci. Technol. 49 (3), 1277–1285.

Kawamura, H., Kobayashi, T., Furuno, A., In, T., Ishikawa, Y., Nakayama, T., Shima, S., Awaji, T., 2011. Preliminary numerical experiments on oceanic dispersion of ^{131}I and ^{137}Cs discharged into the ocean because of the Fukushima Daiichi nuclear power plant disaster. J. Nucl. Sci. Technol. 48, 1349–1356.

Keum, D.-K., Jun, I., Kim, B.-H., Lim, K.-M., Choi, Y.-H., 2015. A dynamic model to estimate the activity concentration and whole body dose rate of marine biota as consequences of a nuclear accident. J. Environ. Radioact. 140, 84–94.

Landrum, P.F., Lee, H., Lydy, M.J., 1992. Annual review: toxicokinetics in aquatic systems: model comparison and use inn hazard assessmen. Environ. Toxicol. Chem. 11, 1709–1725.

Lepicard, S., Heling, R., Maderich, V., 2004. POSEIDON/RODOS models for radiological assessment of marine environment after accidental releases: application to coastal areas of the Baltic, Black and North Seas. J. Environ. Radioact. 72, 153–161.

Liebig, J., 1847. Chemistry in its Application to Agriculture and Physiology, fourteenth ed. (London).

Maderich, V., Bezhenar, R., Heling, R., de With, G., Jung, K.T., Myoung, J.G., Cho, Y.-K., Qiao, F., Robertson, L., 2014. Regional long-term model of radioactivity dispersion and fate in the Northwestern Pacific and adjacent seas: application to the Fukushima Dai-ichi accident. J. Environ. Radioact. 131, 4–18.

Min, B.I., Periáñez, R., Kim, I.G., Suh, K.S., 2013. Marine dispersion assessment of ^{137}Cs released from the Fukushima nuclear accident. Mar. Pollut. Bull. 72, 22–33.

Periáñez, R., Brovchenko, I., Duffa, C., Jung, K.-T., Kobayashi, T., Lamego, F., Maderich, V., Min, B.-I., Nies, H., Osvath, I., Psaltaki, M., Suh, K.-S., 2015. A new comparison of marine dispersion model performances for Fukushima Dai-ichi releases in the frame of IAEA MODARIA program. J. Environ. Radioact. 150, 247–269.

Periáñez, R., Suh, K.S., Min, B.I., Casacuberta, N., Masqué, P., 2013. Numerical modelling of the releases of ^{90}Sr from Fukushima to the ocean: an evaluation of the source term. Environ. Sci. Technol. 47, 12305–12313.

Polikarpov, G.G., 1965. Radioecology of Aquatic Organisms: the Accumulation and Biological Effect of Radioactive Substances. North Holland Publishing Co., Amsterdam, p. 314.

Psaltaki, M., Brown, J.E., Howard, B.J., 2013. TRS Cs CR_{wo}-water values for the marine environment: analysis, applications and comparisons. J. Environ. Radioact. 126, 367–375.

Rigas, M.L., 2000. Software review: Modelmaker 4.0. Risk Anal. 20 (4), 543–544.

Rowan, D.J., Rasmussen, J.B., 1996. Measuring the bioenergetic cost of fish activity in situ using a globally dispersed radiotracer (137Cs). Can. J. Fish. Aquatic Sci. 53, 734–745.

Sazykina, T., 2003. Radioactivity in aquatic biota. Chapter 7. In: Scott, E.M. (Ed.), Modelling Radioactivity in the Environment, pp. 201–219.

Sazykina, T.G., 2000. ECOMOD – an ecological approach to radioecological modelling. J. Environ. Radioact. 50 (3), 207–220.

Tateda, Y., Tsumune, D., Tsubono, T., 2013. Simulation of radioactive cesium transfer in the southern Fukushima coastal biota using a dynamic food chain transfer model. J. Environ. Radioact. 124, 1–12.

Thomann, R.V., 1981. Equilibrium model of fate of microcontaminants in diverse aquatic food chains. Can. J. Fish. Aquatic Sci. 38, 280–296.

UNSCEAR, 2014. Sources, effects and risk of ionizing radiation. Volume I: report to the General Assembly, Scientific Annex A: levels and effects of radiation exposure to the nuclear accident after the 2011 great east-Japan earthquake and tsunami. United Nations Scientific Committee on the Effects of Atomic Radiation. In: Report to the 68th Session of the United Nations General Assembly A/68/46, Vienna, 2 April 2014, p. 311.

Vernadsky, V.I., 1929. La Biosphere. Felix Alcan, paris.

Vives Batlle, J., Wilson, R.C., Watts, S.J., Jones, S.R., McDonald, P., Vives-Lynch, S., 2008. Dynamic model for the assessment of radiological exposure to marine biota. J. Environ. Radioact. 99 (1), 1711–1730.

Vives i Batlle, J., 2011. Impact of nuclear accidents on marine biota. Integr. Environ. Assess. Manag. 7 (3), 365–367.

Vives i Batlle, J., 2012. Radioactivity in the marine environment. In: Meyers, R.A. (Ed.), Encyclopaedia of Sustainability Science and Technology. Springer Science & Business Media, LLC, pp. 8387–8425.

Vives i Batlle, J., 2014. Dynamic modelling of radionuclide uptake by marine biota: application to Fukushima assessment. In: Proc. ICRER 2014-3rd International Conference on Radioecology & Environmental Radioactivity, 7-12 September 2014, Barcelona, Spain. Electronic proceedings 10.1. Lessons learnt from the Fukushima accident, Paper O-086. Available from: http://radioactivity2014.pacifico-meetings.com/.

Vives i Batlle, J., 2016. Dynamic modelling of radionuclide uptake by marine biota: application to the Fukushima nuclear power plant accident. J. Environ. Radioact. 151 (2), 502–511.

Vives i Batlle, J., Aono, T., Brown, J.E., Hosseini, A., Garnier-Laplace, J., Sazykina, T., Steenhuisen, F., Strand, P., 2014. The impact of the Fukushima nuclear accident on marine biota: retrospective assessment of the first year and perspectives. Sci. Total Environ. 487, 143–153.

Vives i Batlle, J., Balonov, M., Beaugelin-Seiller, K., Beresford, N.A., Brown, J., Cheng, J.-J., Copplestone, D., Doi, M., Filistovic, V., Golikov, V., Horyna, J., Hosseini, A., Howard, B.J., Jones, S.R., Kamboj, S., Kryshev, A., Nedveckaite, T., Olyslaegers, G., Pröhl, G., Sazykina, T., Ulanovsky, A., Vives-Lynch, S., Yankovich, T., Yu, C., 2007a. Inter-comparison of unweighted absorbed dose rates for non-human biota. Radiat. Environ. Biophys. 46 (4), 349–373.

Vives i Batlle, J., Barnett, C.L., Beaugelin-Seiller, K., Beresford, N.A., Copplestone, D., Horyna, J., Hosseini, A., Johansen, M., Kamboj, S., Keum, D.-K., Newsome, L., Olyslaegers, G., Vandenhove, H., Vives Lynch, S., Wood, M., 2011. Absorbed dose conversion coefficients for non-human biota: an extended inter-comparison of data. Radiat. Environ. Biophys. 50 (2), 231–251.

Vives i Batlle, J., Vandenhove, H., 2014. Dynamic modelling of the radiological impact of the Fukushima accident on marine biota. Ann. Belg. Ver. Stralingsbescherming 38 (3), 299–312.

Vives i Batlle, J., Wilson, R.C., McDonald, P., 2007b. Allometric methodology for the calculation of biokinetic parameters for marine biota. Sci. Total Environ. 388 (1–3), 256–269.

Vives i Batlle, J., Wilson, R.C., Watts, S.J., Jones, S.R., McDonald, P., Vives-Lynch, S., 2008. Dynamic model for the assessment of radiological exposure to marine biota. J. Environ. Radioact. 99, 1711–1730.

Whicker, F.W., Schultz, V., 1982. Radioecology: Nuclear Energy and the Environment, vol. 1. CRC press, Inc, Boca Raton, Florida.